Genetic Reconstitution of Functional Acetylcholine Receptor Channels in Mouse Fibroblasts

TONI CLAUDIO,* W. N. GREEN, DEBORAH S. HARTMAN, DEBORAH HAYDEN, HENRY L. PAULSON, F. J. SIGWORTH, STEVEN M. SINE, ANNE SWEDLUND

Foreign genes can be stably integrated into the genome of a cell by means of DNA-mediated gene transfer techniques, and large quantities of homogenous cells that continuously express these gene products can then be isolated. Such an expression system can be used to study the functional consequences of introducing specific mutations into genes and to study the expressed protein in the absence of cellular components with which it is normally in contact. All four *Torpedo* acetylcholine receptor (AChR) subunit complementary DNA's were introduced into the genome of a mouse fibroblast cell by DNA-mediated gene transfer. A clonal cell line that stably produced high concentrations of correctly assembled cell surface AChR's and formed proper ligand-gated ion channels was isolated. With this new expression system, recombinant DNA, biochemical, pharmacological, and electrophysiological techniques were combined to study *Torpedo* AChR's in a single intact system. The physiological and pharmacological profiles of *Torpedo* AChR's expressed in mouse fibroblast cells differ in some details from those described earlier, and may provide a more accurate reflection of the properties of this receptor in its natural environment.

THE NICOTINIC ACETYLCHOLINE RECEPTOR IS THE LIGAND-gated ionic channel that binds the neurotransmitter acetylcholine (ACh) and mediates synaptic transmission between nerve and muscle. It is located in the postsynaptic membrane of the vertebrate neuromuscular junction and is composed of four different polypeptide chains with the stoichiometry $\alpha_2\beta\gamma\delta$. A particularly rich source of acetylcholine receptor (AChR) for biochemical studies is the electric organ of the marine ray *Torpedo*, and the AChR from this tissue has been the most intensively studied in terms of its structure, ligand-binding properties, and conformational transitions (*1*). However, the morphology of the *Torpedo* electric organ has prevented in situ cell biological and functional studies of the AChR such as biosynthesis, assembly, modulation, flux, and ligand binding. Instead, our knowledge of the functional properties of *Torpedo* AChR's has come entirely from studies on membrane fragments or on AChR's reconstituted into artificial membrane systems, and, most recently, from the transient expression of AChR's in *Xenopus laevis* oocytes with in vitro synthesized messenger RNA (mRNA) transcribed from wild-type and mutated complementary DNA's (cDNA's) (*2–4*). This last technique has been used to great advantage in studying the functional consequences of specific mutations in the AChR cDNA's. However, studies with the oocyte expression system are limited in the types of questions that can be addressed and in the types of analyses that can be performed. Because proteins are produced only during the lifetime of the injected RNA, studies requiring that AChR's be expressed for more than a few days are not practical in this system. Also, because the cells must be individually injected, only small quantities of AChR can be produced. This latter limitation is particularly significant because a variety of standard pharmacological assays that are necessary to characterize cloned receptors and channels cannot be conducted in the oocyte system.

As an alternative, we have pursued the stable expression of *Torpedo* AChR's by introducing the four AChR subunit cDNA's into the genomes of cultured cell lines. With this system, large numbers of identical cells are readily obtained that are amenable to biochemical, cell biological, pharmacological, and physiological characterization. We now report here the first stable expression of a protein of this complexity, obtained by cotransfecting the four AChR subunit cDNA's and a selectable marker gene into mouse fibroblast cells. We show that the subunits were assembled into complexes of the proper size and inserted into the plasma membrane where they are fully functional. Ligand-binding studies and electrophysiological recordings from *Torpedo* AChR's in the same intact cells are presented. The pharmacological and physiological data collected thus far suggest that our stable expression system may more closely parallel the native *Torpedo* membrane environment than other systems used to characterize *Torpedo* AChR's. We also found, quite unexpectedly, that expression of functional *Torpedo* AChR's in mouse fibroblasts was strongly temperature sensitive.

Expression system. Although DNA-mediated gene transfer by the calcium phosphate precipitation method is inefficient for the stable introduction of material into the genome of cells (about one transfectant in 10^3 to 10^5 cells), cells that have integrated a selectable marker gene can be readily identified, and co-introducing a gene or cDNA with that selectable marker can be very effective (*5*). In order to express a multisubunit protein such as the AChR, four different

T. Claudio, W. N. Green, D. Hayden, F. J. Sigworth, S. M. Sine, and A. Swedlund are in the Department of Cellular and Molecular Physiology, Yale University School of Medicine, 333 Cedar Street, New Haven, CT 06510. D. S. Hartman is in the Department of Biology, Yale University, 219 Prospect Street, New Haven, CT 06511. H. V. Paulson is in the Department of Cell Biology, Yale University School of Medicine, 333 Cedar Street, New Haven, CT 06510.

*To whom correspondence should be addressed.

cDNA's must be introduced into the same cell. We recently showed that 80 percent of fibroblast cells that integrated a selectable marker gene also integrated copies of the four subunit cDNA's (*4*). In our study, we have engineered the four *Torpedo* AChR cDNA's (*4*, *6*) into a simian virus 40 (SV40) expression vector. Murine fibroblast L cells deficient in thymidine kinase (tk^-) and adenine phosphoribosyltransferase (Ltk^-aprt^-) were transfected with these DNA's plus a *tk* gene (*7*) by calcium phosphate precipitation (*8*, *9*). The tk^+ transformants were put into selective medium, and 11 colonies were isolated with the use of cloning cylinders, and grown into stable cell lines. One of these cell lines, "all-11," is described below.

Characterization of integrated DNA. DNA from the all-11 cell line was subjected to Southern blot analysis (*10*, *11*) in order to determine the integrity and the copy number of each of the integrated cDNA's. By comparing the sizes of the cDNA's integrated into the genome with the starting plasmid DNA's (Fig. 1), it appeared that the majority of the subunit cDNA's were integrated intact. A comparison of the intensities of the α, β, γ, and δ bands with that of an integrated single copy cDNA [an α cDNA introduced into NIH 3T3 cells with a retrovirus recombinant and viral infection (*12*)] indicated that the copy number for each of the cDNA's was approximately 4:2:2:8 for α, β, γ, and δ, respectively. The observations that most of these DNA's were correctly integrated and that the copy numbers varied somewhat, are consistent with our earlier report (*4*) in which the integrated cDNA's from 11 cell lines were analyzed after cotransfection of the four *Torpedo* AChR subunit cDNA's and *aprt*.

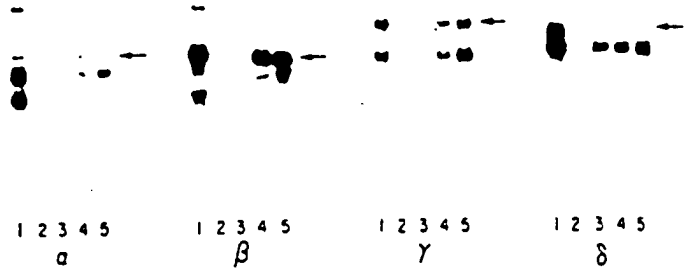

Fig. 1. DNA blots of the all-11 cell line. Genomic DNA's probed with α, β, γ, and δ sequences are marked α, β, γ, and δ; the plasmid preparations digested with the same restriction enzymes as the genomic DNA are preceded by "p." The transfecting DNA's were prepared as follows. The dihydrofolate reductase gene was removed from the vector pSV2-DHFR (*40*) with a Hind III–Bgl II digestion, and a single Bgl II cloning site was created with Bgl II linkers (1001, New England Biolabs). The full-length α and β clones were isolated from our *Torpedo californica* electric organ λgt10 cDNA library (*4*) with Eco RI digestions, the 1625–base pair (bp) Nco I to Pvu II fragment from the γ clone (*6*) and the ~1770-bp Sac I to 3′ Eco RI linker fragment from our δ clone (*4*) were also isolated. The ends of all of these inserts were filled in with the Klenow fragment of DNA polymerase I, and Bcl I linkers (1009, New England Biolabs) were phosphorylated with polynucleotide kinase and ligated to the termini. Each of these cDNA's was inserted into the Bgl II cloning site of pSV2. Ltk^-aprt^- cells were transfected with these DNA's by the calcium phosphate precipitation procedure of Graham and van der Eb (*8*) as modified by Wigler *et al.* (*9*). The plasmid (*7*) ptk (50 μg) and 5 μg each of pSV2-α, pSV2-β, pSV2-γ, and pSV2-δ were introduced into 5×10^5 Ltk^-aprt^- cells on 10-cm plates (*4*). Tk^+ transformants were selected in Dulbecco's modified Eagle's medium (DMEM) containing 10 percent calf serum and hypoxanthine at 15 μg/ml, aminopterin at 1 μg/ml, and thymidine at 5 μg/ml (1× HAT). Genomic DNA was prepared from a confluent 10-cm dish of cells (*41*). DNA that would be probed for α, β, and δ sequences was digested with Sty I (New England Biolabs). DNA to be probed for γ sequences was digested with Pvu II and Eco RI. Digested DNA (5 μg) was loaded onto 1 percent agarose gels and blotted (*11*). Probes for each of the cDNA's were as follows. A 1090-bp Pvu II–Pst I fragment for α; a 700-bp Bgl II fragment for β; a 1290-bp Bgl II–Eco RI fragment for γ, and a 450-bp Hind III fragment for δ. Each was radiolabeled with (^{32}P) by means of the multiprime labeling system (Amersham) (*42*) and had specific activities of ~10 cpm per microgram of DNA.

RNA was isolated from the all-11 cell line and subjected to Northern blot analysis to determine whether transcripts were being made, the sizes of the transcripts, and the relative levels of each. For each subunit, a transcript of the proper size was observed (arrows in Fig. 2). The amount of the different subunit RNA transcripts varied but were consistent with the number of integrated copies of each cDNA (Fig. 1). The explanation of the multiplicity of transcripts has not yet been determined. Because polyadenylylation signals (*13*) in the 3′ untranslated regions of the cDNA's were not removed, the smaller transcripts could be explained if these sites were used for polyadenylylation instead of the site provided in the SV40 vector. It is also possible that the smaller RNA's seen in the α and γ blots were transcribed from incorrectly integrated cDNA's (see Fig. 1). A third possibility is that the smaller transcripts seen in the γ and δ blots were due to aberrant splicing (*14*).

As discussed below, we found that the presence of sodium butyrate (*15*) in the medium and incubation of the cells at temperatures lower than 37°C were both critical for expression of *Torpedo* AChR's in cultured cells. We therefore examined the effects of sodium butyrate and temperature on transcription. The presence of 10 m*M* sodium butyrate for 2 days greatly increased the transcription (Fig. 2, lanes 1 and 2). The temperature effect on some of the transcripts was also noteworthy; for example, a different sized transcript was seen in the δ blot at 37°C (Fig. 1, lane 1) compared with 28°C (lanes 3 to 5).

Expression of toxin binding sites and proper subunit polypeptides. To test for expression of cell surface AChR complexes, we incubated cells with ^{125}I-labeled α-bungarotoxin (BuTx) for 90 minutes, removed the unbound toxin, and counted the cells in a gamma counter. We were unable to detect any toxin binding activity unless all-11 cells were grown in the presence of sodium butyrate and at a reduced temperature (Fig. 3A). The optimum temperature was not determined; but at 28°C, the maximum expression of [^{125}I]BuTx-binding sites expressed on the cell surface was ~52 fmol per 35-mm dish (~12,600 AChR's per cell). The internal pool of BuTx-binding AChR's was small, about 10 percent of the number of surface AChR's. At 28°C, expression reached a peak between days 5 and 7 (Fig. 3A). The decline of AChR expression after cells were cultured for 7 days in sodium butyrate at 28°C was due to cell death caused, in part, by the toxic effects of sodium butyrate on cell viability. Thus, although the cDNA's were stably integrated into the genome of cells and the subunits were expressed constitutively at low levels, transcription was greatly enhanced by the presence of sodium butyrate and expression of functional AChR's was temperature-sensitive, enabling us to regulate AChR expression.

To analyze the expressed proteins, we incubated a confluent 10-cm dish of cells with sodium butyrate for 2 days at 37°C or for 5 days at 28°C. The cells were then metabolically labeled with [^3H]leucine, solubilized, and immunoprecipitated (*12*) with a mixture of antisera to *Torpedo* α, β, γ, and δ (anti-α, -β, -γ, and -δ) (*16*). The labeling pattern was identical for the two incubation conditions and all four of the subunit polypeptides were observed (Fig. 3B). The migration of each of the subunits was the same as that of native AChR subunits isolated from *Torpedo californica* electroplaque tissue, except for the γ subunit. With this subunit, the polypeptide synthesized in mouse fibroblasts appeared to migrate as if it were ~3000 daltons smaller than when synthesized in electroplaque. The altered migration may be due to differences in glycosylation between

mouse and *Torpedo* cells rather than to some difficulty with the γ clone, since all of the clones encode proper AChR subunits (*4*, *12*). Because the γ subunit contains the greatest number of asparagine-linked glycosylation sites [four to five (*6*) compared with one each for α and β, and three for δ (*17*)], one would expect this subunit to be most affected by being processed in a foreign environment (*18*).

In addition to the four AChR subunit bands, four other bands were observed (Fig. 3B)—at ~80 kD, 28 kD, 26 kD, and 20 kD. When dishes of labeled cells were immunoprecipitated separately, with antisera to α, β, γ, and δ subunits, the band at ~80 kD was seen in all lanes indicating that it was precipitated nonspecifically. The band at ~28 kD was recognized only by anti-α and the bands at ~26 kD and ~20 kD were recognized by anti-γ. The subunits were not all produced at the same level but the level of expression was, for the most part, consistent with the level of transcription (Fig. 2) and with the number of integrated cDNA's (Fig. 1).

Subunit composition and stoichiometry. Although our all-11 cell line expressed each of the four AChR subunits, and molecules were capable of binding BuTx, the question remained whether the receptor subunits had associated into proper $\alpha_2\beta\gamma\delta$ complexes. Fujita *et al.* (*19*) presented evidence that, in yeast, transiently expressed *Torpedo* α subunits were inserted into the plasma membrane in the absence of the other subunits and bound BuTx with low affinity ($K_D \sim 10^{-5} M$). However, we found that when a single α subunit cDNA was stably expressed in mammalian cultured cell lines (either fibroblast or muscle cells), α subunits were not inserted into the plasma membrane although these internally expressed α subunits were capable of low-affinity BuTx binding (*12*). Because our assays were performed with nanomolar concentrations of toxin such that low affinity toxin binding would not be detected, and because α subunits are not expressed on the surface of this system, our results suggested that the BuTx binding we were observing on the surface of all-11 cells was not due to toxin binding to isolated α subunits. That AChR complexes were indeed formed was demonstrated directly by measuring the sedimentation coefficient of the BuTx-binding material. If the subunits had associated into proper $\alpha_2\beta\gamma\delta$ pentamers, then the molecules should migrate on sucrose gradients with a sedimentation coefficient of 9*S* (~250 kD) (*1*). A plate of all-11 cells was surface labeled with [^{125}I]BuTx, solubilized in a buffer containing 1 percent Triton X-100, and layered onto 5 to 20 percent sucrose gradients. The [^{125}I]BuTx-binding material migrated at 9*S* (Fig. 3C), and comigrated precisely with the 9*S* "monomeric" peak of AChR produced in electroplaque.

In *Torpedo*, unlike any other source of AChR, AChR's also exist as disulfide linked "dimers" that migrate at 13*S* (~500 kD) (*1*). When treated with reducing agents, AChR dimers are converted to the 9*S* form. We harvested AChR's from all-11 cell lines and analyzed them on sucrose gradients in the presence and absence of dithiothreitol (Fig. 3C). Under either condition, the *Torpedo* AChR's isolated from mouse fibroblast cells always migrated as monomeric 9*S* complexes. We do not know whether some other component present in *Torpedo* electroplaque tissue is required for the formation of AChR dimers or whether the lack of dimers is due simply to the low surface density of AChR's in our system compared with the density in electroplaque (~15/μm^2 compared with 10^4/μm^2).

Pharmacological characterization. We were able to harvest large

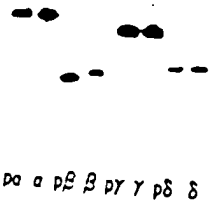

Fig. 2. RNA blots of all-11 cells showing temperature and sodium butyrate effects on transcription. The arrows indicate the transcripts that were polyadenylylated with the use of signals provided in the SV40 vector. When a 10-cm dish of cells was just confluent (~10^7 cells), the medium was replaced with DMEM containing 10 percent calf serum, 1× HAT, and 10 m*M* sodium butyrate (SB medium), and the cells were either grown for 2 days at 37°C and 5 percent CO_2 (lane 1) or moved to an incubator maintained at 28°C and 5 percent CO_2 (lanes 2 to 5). Cells were harvested after 0 (lane 2), 2 (lane 3), 5 (lane 4), or 6 (lane 5) days at 28°C. RNA was prepared according to Chirgwin *et al.* (*43*). RNA (10 μg) was subjected to electrophoresis on 1% agarose gels and blotted according to standard procedures (*10*) with the use of the same subunit-specific cDNA probes described in the legend to Fig. 1.

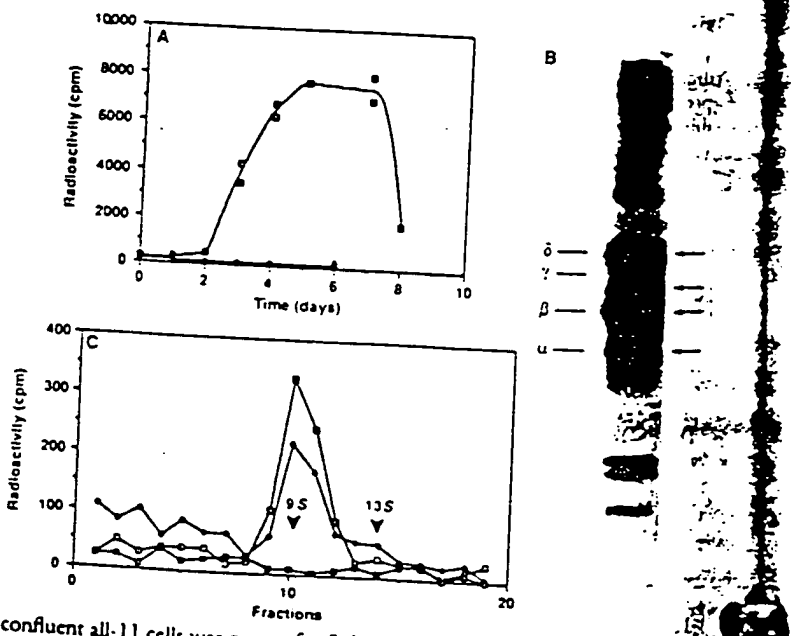

Fig. 3. Expression of *Torpedo* AChR's in mouse fibroblast cells. (**A**) Time course of surface AChR expression in all-11 cells. All-11 cells were grown in 35-mm dishes at 37°C in DMEM, 10 percent calf serum, and 1× HAT until just confluent. Sodium butyrate (10 m*M*) was added, and the cells were either kept at 37°C (filled squares) or were moved to an incubator maintained at 28°C (open squares) for 0 to 8 days. Dishes were labeled in 740 μl of phosphate-buffered saline (PBS) containing 0.03 percent bovine serum albumin (BSA) and 0.35 n*M* [^{125}I]BuTx (1000 cpm/fmol) for 90 minutes, washed three times in 5 ml in PBS-BSA, solubilized in 1.0 ml of 1.0 percent Triton X-100, and counted in a gamma counter (**B**) Subunit expression in all-11 cells. The positions of AChR subunits isolated from *Torpedo californica* electroplaque tissue are marked α, β, γ, and δ. Arrows indicate the positions of *Torpedo* subunits isolated from all-11 cells. A 10-cm dish of cells was grown for 2 days at 37°C in SB medium (see legend to Fig. 2). The cells were incubated in leucine-depleted medium for 15 minutes and then 400 μCi of [^{3}H]leucine (Amersham) was added, and labeling continued for 20 minutes. The cells were next harvested, solubilized in a buffer containing 1 percent Triton X-100, incubated with a mixture of antisera to *Torpedo* α, β, γ, and δ, followed by Protein A–Sepharose (Sigma) (*12*). Immunoprecipitates were analyzed on 10 percent SDS-polyacrylamide gels and treated for fluorography. (**C**) Sedimentation coefficient of *Torpedo* AChR's expressed in mouse fibroblasts. The filled diamonds indicate the profile of all-11 cells labeled with [^{125}I]BuTx in the presence of 10 m*M* dithiothreitol; the open squares indicate the profile of all-11 cells labeled with [^{125}I]BuTx in the absence of dithiothreitol; the filled squares indicate the profile of all-11 cells that were first incubated with 20 m*M* carb and then labeled with [^{125}I]BuTx in the continued presence of carb; the arrows mark the position of the 9*S* monomeric and 13*S* dimeric AChR complexes isolated from *Torpedo* electroplaque tissue (determined by running a parallel gradient of *Torpedo* electroplaque AChR's labeled with [^{125}I]BuTx). A 10-cm dish of confluent all-11 cells was grown for 5 days at 28°C is SB medium. Cells were incubated for 90 minutes with [^{125}I]BuTx, harvested in a Triton X-100 containing buffer, centrifuged on 13-ml sucrose gradients (5 to 20 percent), and 0.6-ml fractions were collected. Portions (50 μl) of each fraction were counted in a gamma counter, and the profiles are shown in (C).

quantities of the all-11 clonal cell line to examine the pharmacological properties of *Torpedo* AChR's expressed in intact cells. The overall pharmacological profile was qualitatively similar to that determined for AChR's in membrane fragments of *Torpedo* electroplaque and for AChR's in intact cells from the mouse muscle cell line, BC_3H-1 (*20*). The agonist binding properties were, however, quantitatively different from those of *Torpedo* membranes, but closely matched those of intact BC_3H-1 cells.

The kinetics of [^{125}I]BuTx binding to intact all-11 cells were examined (Fig. 4, A and B). The time course of association revealed that BuTx bound with high specificity with a forward rate constant of $2.2 \pm 0.3 \times 10^5\ M^{-1}\ sec^{-1}$ (±SE). This rate constant was close to that estimated for BuTx binding to *Torpedo* AChR membranes (*21*) and for α-neurotoxin binding to AChR's of intact BC_3H-1 cells (*20*). Toxin dissociated very slowly (Fig. 4B), with a rate constant of $1.75 \pm 0.13 \times 10^{-5}\ sec^{-1}$ (±SE). This dissociation rate was comparable to that for intact BC_3H-1 cells (*22*), but was about twice that for *Torpedo* AChR membranes (*23*). The ratio of dissociation to association rate constants gave a dissociation constant of $7.8 \times 10^{-11} M$.

Receptor occupancy by unlabeled agonists and antagonists was examined by their competition against the initial rate of [^{125}I]BuTx binding (*21*). The competition against toxin binding for the classical antagonist, dimethyl-*d*-tubocurarine (DMT) is shown in Fig. 4C. Fitted by the empirical Hill equation (*24*), the competition curve is described by a dissociation constant of 2.5 μ*M* and a Hill coefficient of 0.69. The less-than-unity Hill coefficient is consistent with measurements from BC_3H-1 cells (*20, 25*) and *Torpedo* membrane fragments (*26*) which show that reversible antagonists exhibit different affinities for the two binding sites on the receptor. Analyzed according to the two-site model (*25*), the competition data reveal dissociation constants of 0.52 μ*M* and 12.0 μ*M*. This asymmetry seen in dissociation constants is similar to the asymmetry seen for BC_3H-1 (0.3 μ*M* and 28 μ*M* (*25*) and *Torpedo* (0.5 μ*M* and 10 μ*M*) (*26*) AChR's.

Toxin is displaced in the presence of the agonists ACh and carbamylcholine (carb) (Fig. 4D). The competition curves are described by dissociation constants K_D = 0.71 and 10 μ*M* and Hill coefficients n_H = 1.48 and 1.25 for ACh and carb, respectively. The relative affinities of these agonists are similar to those determined for AChR's from *Torpedo* membranes. The absolute dissociation constants are however 20 to 30 times greater and the Hill coefficients are larger than those measured (*27*) in *Torpedo* membranes [K_D = 0.024 (ACh) and 0.5 μ*M* (carb); n_H = 1.1(carb)]. The difference in binding parameters can be accounted for (*28*) by a larger allosteric constant in the *Torpedo* membrane preparation, representing a shift of the allosteric equilibrium toward the high-affinity, desensitized state of the AChR. That this shift may be due to membrane disruption is suggested by the difference in binding of carb in intact BC_3H-1 cells (K_D = 11 μ*M*, n_H = 1.5) and in membrane fragments from these cells [K_D = 1 μ*M*, n_H = 1.0 (*29*)]. Thus, it may be that our expression system allows us to measure ligand-binding properties of the *Torpedo* AChR that more closely reflect those of its native environment.

Functional characterization. Initially, a ^{22}Na flux assay was used to demonstrate that cell surface AChR complexes facilitated ion flux into cells in response to agonist. ACh at 60 μ*M* induced a rapid uptake of ^{22}Na, and this uptake was reduced to identical background levels by prior incubation with 100 n*M* BuTx, 100 μ*M* DMT, or prior exposure to 60 μ*M* ACh (Fig. 5A). ACh-induced tracer uptake thus demonstrated expected pharmacological properties of AChR's, such as susceptibility to block by BuTx and DMT, and ACh-induced desensitization.

Whole-cell current recordings (*30*) also showed an ACh-activated response. The response of an all-11 cell to a "puff" of 30 μ*M* ACh is shown in Fig. 5B. At a membrane potential of −40 mV, application of ACh elicited a rapid inward current of −50 pA which, in the continued presence of ACh desensitized with a time constant of 3.5

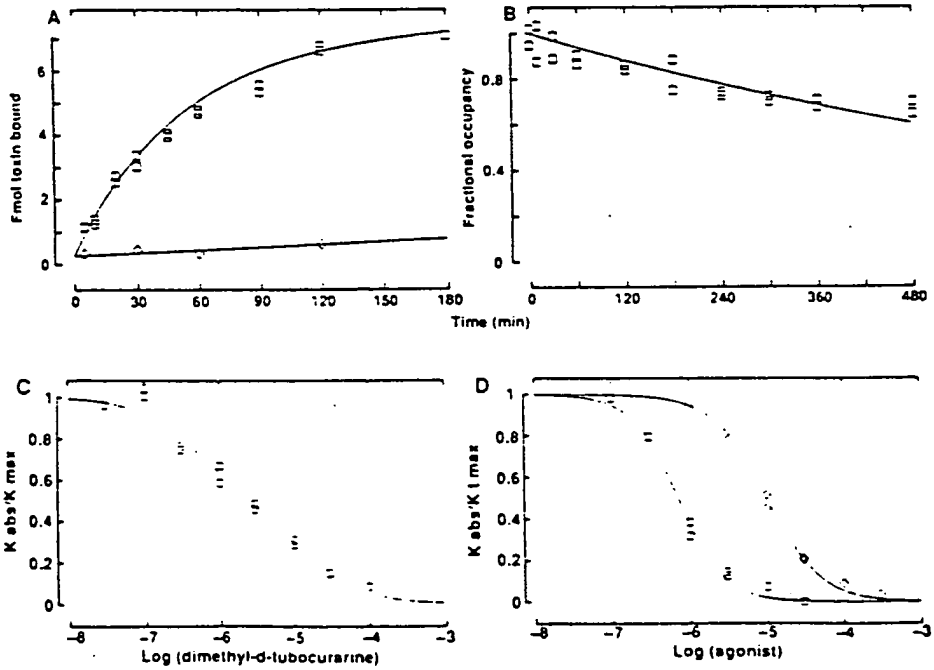

Fig. 4. Pharmacological properties of the *Torpedo* AChR's in all-11 cells. (**A**) Time course of α-bungarotoxin association. After the growth medium was aspirated, all-11 cells were covered with normal mammalian saline (140 m*M* NaCl, 2.5 m*M* KCl, 10 m*M* Hepes, 1.8 m*M* $MgCl_2$, *p*H 7.4) containing [^{125}I]BuTx (1.62 n*M*), and bound toxin was measured at the specified times. The squares represent binding measured in the presence of toxin alone, while the diamonds show nonspecific binding measured with toxin in the presence of 10 m*M* carb. A least-squares fit of the specific binding component yielded a maximum binding of 6.4 fmol and an association rate of $2.25 \times 10^5 M^{-1}\ sec^{-1}$. (**B**) Time course of BuTx dissociation. The fractional occupancy is plotted as the ratio of specific toxin-receptor complexes at the indicated time to the specific complexes immediately after removal of unbound toxin. The curve represents the least-squares fit to fractional occupancy = $\exp(-k_{diss}t)$ where the fitted dissociation rate constant k_{diss} is $1.75 \times 10^{-5}\ sec^{-1}$. (**C**) Competition between DMT and BuTx. Cells were exposed to the specified concentrations of DMT for 30 minutes, and then the initial rates of toxin binding were measured for 30 minutes. The curve is the least squares fit to the two-site model (*25*) with the following parameters: K_A = 0.52 μ*M*, K_B = 12.0 μ*M*. In this experiment the total number of toxin sites was 15.1 fmol per 35-mm dish. (**D**) Competition between agonists and BuTx. Cells were incubated with the specified concentrations of either ACh (diamonds) or carb (squares) for 30 minutes, and then the initial rates of toxin binding were measured by incubation with toxin (0.98 n*M*) for 30 minutes; k_{obs} is the toxin association rate constant in the presence of ligand, and k_i is the rate constant in the absence of ligand. The rate constants were calculated as described (*20*). The curves represent least-squares fits to the Hill equation with the following fitted parameters: for ACh, K_D = 0.71 μ*M* and n_H = 1.48; for carb, K_D = 9.95 μ*M* and n_H = 1.25. The total number of toxin sites was 15.1 fmol per 35-mm dish.

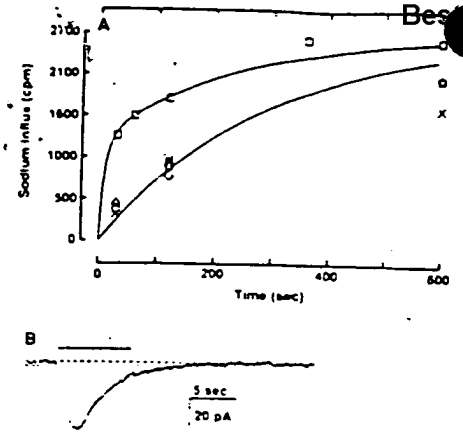

Fig. 5. Functional studies. (**A**) Time course of ACh-induced tracer sodium uptake by all-11 cells. Squares represent ^{22}Na uptake after the instantaneous addition of 60 μM ACh in normal mammalian saline; diamonds are the uptake after 30 minutes of prior exposure to 60 μM ACh; crosses are the uptake measured following the instantaneous addition of 60 μM ACh, but with cells treated with 100 nM BuTx for 30 minutes; triangles are uptake measured in the presence of 100 μM DMT and 60 μM ACh; and the lower squares are the uptake measured in the absence of ACh. The curve through the squares (instantaneous ACh addition) is the visual fit to: cpm $(t) = A_0\{1 - \exp[-k_g(t)]\}$, where $k_g(t) = k_0/k_D[1 - \exp(-k_D t)] + k_{Ft}$ (*44*); k_0 is the permeability shut-off by desensitization; k_F is the permeability resistant to desensitization; and k_D is the rate constant of desensitization onset. The fitted parameters are $k_0 = 0.054$ sec^{-1}, $k_F = 0.0042$ sec^{-1}, and $k_D = 0.081$ sec^{-1}. The lower curve is fitted with the following parameters: $k_0 = 0$, $k_F = 0.0035$ sec^{-1}, and $k_D = 0$. In this experiment, the total number of toxin sites was 8.4 fmol per 35-mm dish of cells. (**B**) Current response of an all-11 cell to the application of ACh, which was applied (at 30 μM) by pressure ejection from a 1-μm pipette for 7 seconds (indicated by the horizontal bar). The downward deflection of the current trace during the ACh puff indicates an increased inward current from the holding current level of −14 pA (dashed line). The dotted curve shows the fit of a single exponential to the decay of the current with a time constant of 3.5 seconds. All-11 cells were grown in 35-mm dishes at 28°C for 7 days in SB medium. Before recording, the medium was replaced with normal mammalian saline plus 1 μM atropine. The pipette solution was 142 mM CsCl, 5 mM NaCl, 2 mM $MgCl_2$, 1 mM EGTA, 10 mM Hepes, pH 7.4. The trace was recorded in the whole cell configuration (*30*) at room temperature, the cell membrane capacitance was 44 pF.

seconds. This desensitization rate is similar to the slow desensitization rate observed for AChR's in both native and reconstituted membranes (*31*). A fast desensitization process (time constant ~100 msec) has also been detected (*31*). However, because our agonist application was not sufficiently fast and uniform, we would not expect to resolve the onset of fast desensitization.

Single channel recordings from all-11 cells showed ACh-induced current pulses having the properties expected for single *Torpedo* AChR currents. In cell-attached recordings obtained with 2 μM ACh in the recording pipette, pulses of inward current lasting ~1 msec and having the amplitude expected for AChR channels were observed (Fig. 6A). To verify that these events arose from ACh-activated channels, we used outside-out patch recordings (*30*) in which currents could be recorded before and during the application of ACh. In a patch obtained from cells showing 19 fmol of BuTx sites per 35-mm culture dish, a flat baseline level of current was observed before and immediately after ACh was added to the bath solution (Fig. 6B), but a high level of channel activity appeared as ACh reached the membrane patch (Fig. 6B). A stretch of this recording 5 minutes later (after desensitization had decreased the frequency of channel openings and thus the probability of overlapping events) was used for quantitative analysis. Amplitude histograms (Fig. 6C) showed a single class of events, whose current-voltage curve (Fig. 6D) gave a slope conductance of 29 pS at 15°C. This level of conductance, and the saturation of current at large negative potentials, are consistent with measurements on *Torpedo* AChR's in oocytes when the lower permeability of Na^+ and block by Mg^{2+} are taken into account (*29*, *32*). The conductance also lies within the range of reported values in reconstituted systems [28 pS (*33*) and 41 pS (*34*); both obtained with Na^+ and at room temperature]. Cell-attached recordings in which Cs^+ carried the inward current showed larger single-channel currents (Fig. 6A), as would be expected from the selectivity of the *Torpedo* AChR.

The record was also analyzed to estimate the mean channel open

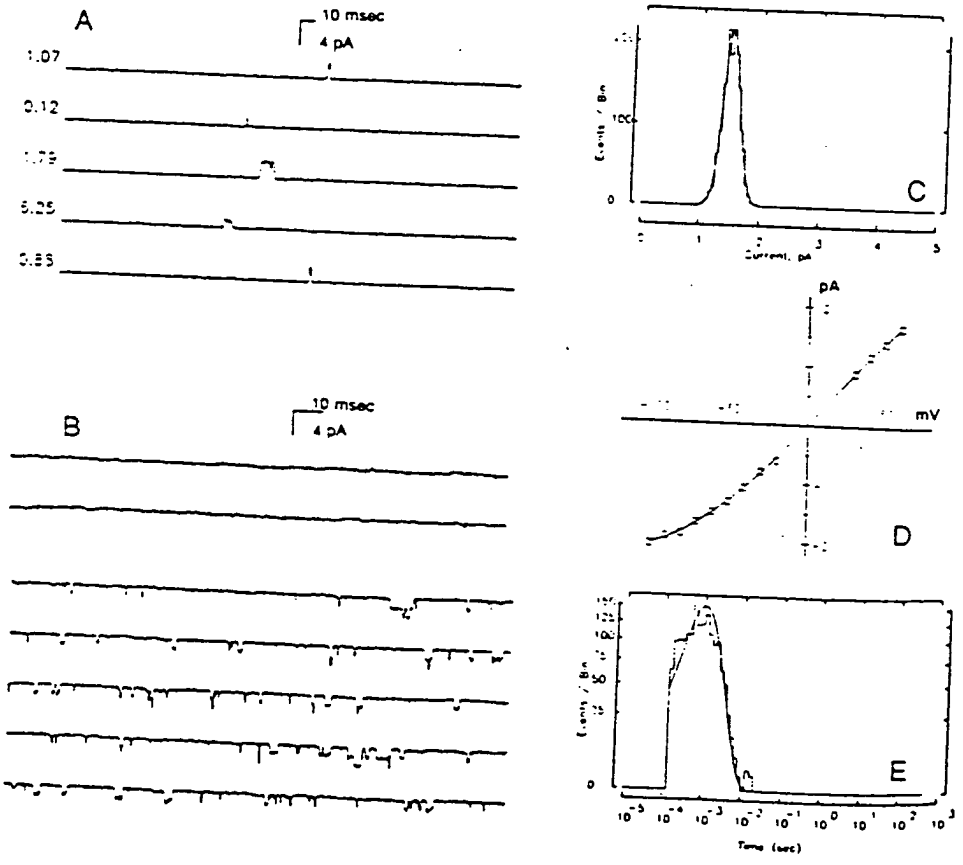

Fig. 6. Single channel recordings from all-11 cells. (**A**) Cell-attached recording with the pipette held at +50 mV and containing a Cs^+, Mg^{2+} solution (in mM: 150 CsCl, 5.4 KCl, 2 $MgCl_2$, 1 EGTA, 10 Hepes; pH 7.4) at 15.5°C. Inward currents are plotted upward and numbers to the left indicate the silent intervals (in seconds) between events. In this recording about 10 percent of the events had a low amplitude (as in the fourth trace). (**B**) Recordings from an outside-out patch at −60 mV and 15.5°C. The first two traces were obtained immediately after ACh was added to the bathing solution. The last five traces are from the same recording 5 seconds later, after ACh has diffused from the point of application to the membrane. ACh was added to a final bath concentration of 2 μM in normal mammalian saline; the pipette solution (in contact with the inside of the membrane) was the same Cs^+ solution as in (A). (**C**) Step amplitude histogram obtained from events longer than 0.5 msec in a later part of the recording shown in (B) at −60 mV. The amplitudes cluster into a single peak at −1.50 ± 0.1 pA (SD) and no low-amplitude events were observed in this outside-out patch. (**D**) Single channel current-voltage (i-V) relation. Points were obtained from fits to distributions as in (C); the curve is a quartic polynomial fit. The slope conductance at 0 mV was 29 pS. (**E**) Open-time distribution from the outside-out patch at −60 mV. The smooth curve is a fitted single-exponential distribution (time constant 1.0 msec) transformed to correspond to the logarithmically binned histogram (*45*).

duration. The distribution of open durations is reasonably described by a single exponential (Fig. 6E) with a time constant of 1 msec. Since only one in ten openings showed brief duration closures, the mean open time is essentially the same as the mean burst duration, and it corresponds closely to that measured for *Torpedo* receptors expressed in *Xenopus* oocytes. A small excess of brief duration openings is also seen (not fitted); brief openings have been observed for most AChR's from skeletal muscle. In sum, the single-channel properties of the *Torpedo* AChR expressed in all-11 cells appear to be the same as those of this same AChR expressed in *Xenopus* oocytes.

Prospects. If a fully functional nicotinic AChR is to be expressed, four different subunits must be correctly processed and assembled into an $\alpha_2\beta\gamma\delta$ pentameric complex. Although DNA mediated gene transfer is an inherently inefficient process, we have shown that the simultaneous introduction of all four cDNA's along with a selectable marker gene into the genome of mouse fibroblast cells can be achieved with high efficiency (*4*). Even though different copy numbers of each cDNA were introduced into the all-11 cell line and different levels of transcription and protein expression were observed, AChR subunits were assembled into proper complexes, and the complexes were inserted into the plasma membrane where they were fully functional. Thus, this method of gene transfer appears to be suitable for introducing genes or cDNA's of proteins into cells that are composed of multiple subunits.

The *Torpedo* AChR's expressed in fibroblasts have the same general characteristics as *Torpedo* AChR's studied in other systems. Our electrical recordings on all-11 cells show ACh-activated channels having desensitization kinetics, single-channel conductance, and lifetimes similar to those already seen in the transient expression of *Torpedo* AChR's in *Xenopus* oocytes. In addition, our stable expression system has allowed us to perform ligand-binding and competition experiments that until now have only been possible with membrane fragment preparations. Like the results from those preparations, we observe the same rank order of affinity of agonists and antagonists, find that antagonists exhibit different affinities for the two ACh binding sites, and observe high-affinity binding of BuTx ($K_D = 7.8 \times 10^{-11} M$).

One difference that we have observed in toxin-displacement experiments is that the equilibrium binding of ACh and carb have larger dissociation constants and Hill coefficients than have been reported in *Torpedo* membrane fragments. When interpreted in terms of an allosteric model for desensitization of the AChR, the weaker binding in the all-11 cells represents a shift of the allosteric equilibrium away from the desensitized state. Whereas in membrane fragment preparations 10 to 30 percent of the AChR's are in the desensitized state in the absence of agonist (*27, 31*), our binding parameters, which are very close to those obtained for AChR's in the mammalian cell line BC_3H-1, would predict that only $\sim 10^{-4}$ of the receptors are desensitized in the absence of agonist. It could be argued that the foreign membrane environment of the all-11 cells shifts the allosteric equilibrium away from the naturally high level of desensitization in a *Torpedo* AChR to a level similar to that of mammalian AChR's. However, we favor the opposite conclusion, that the all-11 cell line is providing us the first view of the *Torpedo* AChR's true ligand-binding properties in an intact membrane. In membrane fragments, the observed high level of resting desensitization could likely have arisen through the procedure of membrane disruption, as appeared to be the case in a study with BC_3H-1 membrane fragments (*29*). Whatever the interpretation of the weaker agonist binding that we observe, the ability to measure the binding is in itself an example of the advantage of the stable expression system, which has already permitted us to perform experiments that would have been impossible to carry out with transient expression in *Xenopus* oocytes.

Another advantage of this stable expression system is that we can now begin to study aspects of the cell biology of the AChR that have been impossible to address in electrocytes or *Xenopus* oocytes, such as assembly, modulation, and nerve-induced clustering. The temperature sensitive effect on assembly, in particular, may prove valuable in studies of the assembly process. Certain structural studies might also be best performed with our expression system. For example, having large quantities of AChR's expressed on the surface of cultured cells will allow easy access to surface subunit epitopes by monoclonal antibodies directed against different structural and functional domains (*35*). This line of experimentation may help to define the topology of folding of the individual subunits in the plane of the membrane (*6, 36*) and thus provide more insight into predicting the folding patterns of transmembrane domains of proteins from hydropathy profiles (*37*). Such information will not only be of use in determining the AChR subunit topology, but it is likely to also be applicable to studies of other closely related proteins such as the ligand-gated glycine (*38*) and γ-aminobutyric acid (*39*) (GABA) receptor-channels.

REFERENCES AND NOTES

1. D. M. Fambrough, *Physiol. Rev.* 59, 165 (1979); A. Karlin, *The Cell Surface and Neuronal Function*, C. W. Cotman, G. Poste, G. L. Nicolson, Eds. (North-Holland, Amsterdam, 1980), vol. 6, p. 191; B. M. Conti-Tronconi and M. A. Raftery, *Annu. Rev. Biochem.* 51, 491 (1982); J.-L. Popot and J.-P. Changeux, *Physiol. Rev.* 64, 1162 (1984); J. O. Dolly and E. A. Barnard, *Biochem. Pharmacol.* 33, 841 (1984); R. Anholt, J. Lindstrom, M. Montal, *The Enzymes of Biological Membranes*, A. Martonosi, Ed. (Plenum, New York, 1984), vol. 3, p. 335; M. P. McCarthy, J. P. Earnest, E. F. Young, S. Choe, R. M. Stroud, *Annu. Rev. Neurosci.* 9, 383 (1986); T. Claudio, *Trends Pharmacol. Sci.* 7, 308 (1986); A Maelicke, in *Handbook of Experimental Pharmacol*, V. P. Whittaker, Ed. (Springer-Verlag, New York, in press), the volume title is *The Cholinergic Synapse*.
2. M. Mishina *et al.*, *Nature (London)* 313, 364 (1985).
3. M. M. White, K. Mixter-Mayne, H. A. Lester, N. Davidson, *Proc. Natl. Acad. Sci. U.S.A.* 82, 4852 (1985).
4. T. Claudio, *ibid.* 84, 5967 (1987).
5. R. Kucherlapati, Ed., *Gene Transfer* (Plenum Press, New York, 1986).
6. T. Claudio, M. Ballivet, J. Patrick, S. Heinemann, *Proc. Natl. Acad. Sci. U.S.A.* 80, 1111 (1983).
7. D. M. Robins, R. Axel, A. S. Henderson, *J. Mol. Appl. Genet.* 1, 191 (1981).
8. F. L. Graham and A. J. van der Eb, *Virology* 52, 456 (1973).
9. M. Wigler *et al.*, *Proc. Natl. Acad. Sci. U.S.A.* 76, 1373 (1979).
10. T. Maniatis, E. F. Fritsch, J. Sambrook, Eds., *Molecular Cloning: A Laboratory Manual* (Cold Spring Harbor Laboratory, Cold Spring Harbor, NY, 1982).
11. E. Southern, *J. Mol. Biol.* 98, 503 (1975).
12. T. Claudio, H. L. Paulson, D. Hartman, S. Fine, F. J. Sigworth, *Curr. Top. Membr. Transp.* 29, in press.
13. N. J. Proudfoot and G. G. Brownlee, *Nature (London)* 263, 211 (1976).
14. T. Claudio, unpublished observation.
15. C. M. Gorman, B. H. Howard, R. Reeves, *Nucleic Acids Res.* 11, 7632 (1983).
16. T. Claudio and M. A. Raftery, *Arch. Biochem. Biophys.* 181, 484 (1977).
17. S. Numa *et al.*, *Cold Spring Harbor Symp. Quant. Biol.* 48, 57 (1983).
18. R. Kornfeld and S. Kornfeld, *Annu. Rev. Biochem.* 54, 631 (1985).
19. N. Fujita *et al.*, *Science* 231, 1284 (1986).
20. S. Sine and P. Taylor, *J. Biol. Chem.* 254, 3315 (1979).
21. M. Weber and J.-P. Changeux, *Mol. Pharmacol.* 10, 1 (1974).
22. C. Hyman and S. C. Froehner, *J. Cell. Biol.* 96, 1316 (1983).
23. G. Weiland, B. Georgia, V. T. Wee, C. R. Chignell, P. Taylor, *Mol. Pharmacol.* 12, 1091 (1976).
24. W. E. Brown and A. V. Hill, *Proc. R. Soc. London B* 94, 297 (1922).
25. S. Sine and P. Taylor, *J. Biol. Chem.* 256, 6692 (1981).
26. R. R. Neubig and J. B. Cohen, *Biochemistry* 18, 5464 (1979).
27. G. Weiland and P. Taylor, *Mol. Pharmacol.* 15, 197 (1979).
28. D. Blangy, H. Buc, J. Monod, *J. Mol. Biol.* 29, 13 (1967).
29. S. Sine, unpublished observation.
30. O. P. Hamill, A. Marty, E. Neher, B. Sakmann, F. J. Sigworth, *Pflugers Arch. Gesamte Physiol. Menschen Tiere* 391, 85 (1981).
31. J. W. Walker, K. Takeyasu, M. G. McNamee, *Biochemistry* 21, 5384 (1982); G. P. Hess, E. B. Pasquale, J. W. Walker, M. G. McNamee, *Proc. Natl. Acad. Sci. U.S.A.* 79, 963 (1982).
32. K. Imoto *et al.*, *Nature (London)* 324, 670 (1986).
33. P. Labarca, J. Lindstrom, M. Montal, *J. Gen. Physiol* 83, 473 (1984).
34. D. W. Tank, R. L. Huganir, P. Greengard, W. W. Webb, *Proc. Natl. Acad. Sci. U.S.A.* 80, 5129 (1983).
35. W. J. LaRochelle, B. E. Wray, R. Sealock, S. C. Froehner, *J. Cell Biol.* 100, 684 (1985).
36. R. H. Guy, *Biophys. J.* 45, 249 (1984); J. Finer-Moore and R. M. Stroud, *Proc.*

Natl. Acad. Sci. U.S.A. 81, 155 (1984); M. Ra... Sargent, J. Lindstrom, *Biochemistry* 25, 2633 (1986...
37. T. P. Hopp and K. R. Woods, *Proc. Natl. Acad. Sci. ...A.* 78, 3824 (1981); J. Kyte and R. F. Doolittle, *J. Mol. Biol.* 157, 105 (1982); D. M. Engelman, T. A. Steitz, A. Goldman, *Annu. Rev. Biophys. Biophys. Chem.* 15, 321 (1986).
38. G. Grenningloh *et al.*, *Nature (London)* 328, 215 (1987).
39. P. R. Schofield *et al.*, *ibid.* 328, 221 (1987).
40. S. Subramani, R. C. Mulligan, P. Berg, *Mol. Cell. Biol.* 1, 854 (1981).
41. A. Pellicer, M. Wigler, R. Axel, S. Silverstein, *Cell* 14, 133 (1978).
42. A. P. Feinberg and B. Vogelstein, *Biochemistry* 132, 6 (1983).
43. J. M. Chirgwin, A. E. Przyb... J. MacDonald, W. J. Rutter, *ibid.* 18, 52... (1979).
44. J. Bernhardt and E. Neumann, *Proc. Natl. Acad. Sci. U.S.A.* 75, 3756 (1978).
45. F. J. Sigworth and S. M. Sine, *Biophys. J.*, in press, 1987.
46. Supported by NIH grants NS 21714 (T.C.) and NS 21501 (F.J.S.) and postdoctoral fellowship award from the American Heart Association 11-108... (W.N.G.) and NIH award NS 07102 (A.S.).

28 September 1987; accepted 17 November 1987

"With all I've learned about psychology recently, establishing who's naughty and who's nice is not as simple as it used to be."

0026-895X/91/040463-010$03.00/0

MOLECULAR PHARMACOLOGY, 40:463-472

Structural and Pharmacological Characterization of the Major Brain Nicotinic Acetylcholine Receptor Subtype Stably Expressed in Mouse Fibroblasts

P. WHITING, R. SCHOEPFER, J. LINDSTROM, and T. PRIESTLEY

Neuroscience Research Centre, Merck Sharp and Dohme Research Laboratories, Harlow, Essex, CM20 2QR UK (P.W., T.P.), University of Pennsylvania, Philadelphia, Pennsylvania 19104 (J.L.), and Zentrum für Molekulare Biologie, Molecular Neurobiology, 6900 Heidelberg, FRG (R.S.)

Received January 24, 1991; Accepted July 1, 1991

SUMMARY

Previously, we purified the predominant subtype of brain nicotinic acetylcholine receptor (AChR), analyzed its structure, and found that it was composed of two kinds of subunit, with sequences encoded by cDNAs termed $\alpha 4$ and $\beta 2$. Here we express these cDNAs from chicken brain in stably transfected fibroblasts. We demonstrate by synthesis that these cDNAs encode subunit polypeptides of the expected sizes, which coassemble to form receptor macromolecules having the same size as native AChRs. Additionally, we demonstrate that the expressed AChRs exhibit the ligand-binding pharmacology of native brain AChRs and function as acetylcholine-gated ion channels.

Nicotinic AChRs from mammalian skeletal muscle and fish electric organs are thought to consist of five homologous subunits [two $\alpha 1$ and one each of β, ϵ (γ in fetal forms), and δ], organized like staves of a barrel around a central cation channel, whose opening is triggered by the binding of ACh (1, 2). The subunit composition, initially determined using biochemical approaches, has been confirmed by expressing functional AChRs transiently in *Xenopus* oocytes (3) and in permanently transfected fibroblasts (4, 5), and assembly of those AChRs has been studied by expressing various combinations of these subunits (6, 7).

Nicotnic AChRs immunoaffinity purified from neurons are thought to consist of only two kinds of homologous subunits, probably similarly arranged around a central cation channel (8–11). There are many candidate cDNAs for subunits of neuronal nicotinic AChR subtypes ($\alpha 2$, $\alpha 3$, $\alpha 4$, $\alpha 5$ and $\beta 2$, $\beta 3$, $\beta 4$. . .), and transient expression in *Xenopus* oocytes of combinations of these subunits results in ACh-gated cation channels ($\alpha 2\beta 2$, $\alpha 3\beta 2$, $\alpha 4\beta 2$, $\alpha 2\beta 4$, $\alpha 3\beta 4$, and $\alpha 4\beta 4$ but not $\beta 3$ or $\alpha 5$ combinations) (12–24). The predominant nicotinic AChR subtype purified from brains was shown by amino-terminal amino acid sequence determination to be composed of subunits corresponding to $\alpha 4$ and $\beta 2$ (18, 25). Their stoichiometry was shown to be $(\alpha 4)_2(\beta 2)_3$ by transient expression in *Xenopus* oocytes (26, 27).

In order to provide an expression system in which the biochemical, pharmacological, and electrophysiological properties of neuronal nicotinic AChRs expressed from subunit cDNAs can be most critically compared with the properties of native AChRs (and studied in greater detail than is usually possible in intact tissue), stably transfected cells would be especially useful. Here, for the first time, we describe such a cell line expressing AChRs synthesized from $\alpha 4$ and $\beta 2$ subunit cDNAs. This recombinant approach confirms our previous analyses of the structure of AChRs purified from brain, by showing that the expressed AChRs have biochemical, pharmacological, and electrophysiological properties expected of native AChRs.

Materials and Methods

Construction of Expression Vectors

pkOE expression vector was derived from pkOneo, the kind gift of Dr. Pam Mellon, Salk Institute, San Diego, CA. The *Eco*RI site in this vector was removed by digestion with *Eco*RI, removal of the 5′ overhang with Klenow polymerase, and religation. The neomycin resistance gene of pkOneo was then removed by digestion with *Hind*III, the 5′ overhang was removed with Klenow polymerase, and *Eco*RI linkers were ligated on, giving pkOE (Fig. 1). pMSGneo was derived from pMSG (Phar-

Research in the laboratory of J. L. was supported by grants from the National Institutes of Health (NS11323), the National Science Foundation (BNS-8819911), The Muscular Dystrophy Association, the California Chapter of the M.G. Foundation, the Council for Tobacco Research, and the Council for Smokeless Tobacco Research.

ABBREVIATIONS: AChR, acetylcholine receptor; ACh, acetylcholine; EGTA, ethylene glycol bis(β-aminoethyl ether)-*N,N,N′,N′*-tetraacetic acid; PBS, phosphate-buffered saline; HEPES, 4-(2-hydroxyethyl)-1-piperazineethanesulfonic acid; PMSF, phenylmethylsulfonyl fluoride; SDS, sodium dodecyl sulfate; MMTV, mouse mammary tumor virus; DMPP, 1,1-dimethyl-4-phenylpiperazinium iodide; DHβE, dihydro-β-erythriodine; PAGE, polyacrylamide gel electrophoresis; bp, base pairs; SV40, simian virus 40; PCR, polymerase chain reaction; DMEM, Dulbecco's modified Eagle's medium; SSPE, standard saline-phosphate-EDTA; mAb, monoclonal antibody.

EXHIBIT A

macia). The ~2500-bp *Hind*III-*Eco*RI fragment of pMSG, containing the *gpt* structural gene and SV40 polyadenylation signals, was replaced by the ~2800-bp fragment of pSV2-neo (28) containing the neomycin resistance gene and SV40 polyadenylation signals. The *Eco*RI site was then removed by restriction digestion, blunt ending with Klenow polymerase, and religation. An *Eco*RI cloning site was then inserted at the *Xho*I cloning site by restriction digestion, removal of the 5′ overhang with Klenow polymerase, and addition of *Eco*RI linkers (Fig. 1).

cDNA pCh 23.1, encoding the β2 structural subunit of chicken brain AChRs, has been previously described (18). The 3′ end of pCh 23.1 contains 192 bp of untranslated region, including a poly(A) tail. This 3′ untranslated region was removed using PCR (29), leaving only the stop codon (Fig. 1). Briefly, oligonucleotide primers around an internal *Bam*HI site (bp 1281 of pCh 23.1) and the stop codon of pCh 23.1 (bp 1545) were synthesized, and PCR was performed as previously described (30), using pCh 23.1 as template. The PCR product was purified on a 1% agarose gel, digested with *Bam*HI, and ligated into *Bam*HI (partial digestion)-*Eco*RV-digested pCh 23.1. The truncated pCh 23.1 was then removed from Bluescript SK⁻ (Stratagene) by *Eco*RI-*Hind*III (in the polylinker) digestion. The *Hind*III overhang was blunt ended with Klenow polymerase, *Eco*RI linkers were added, and the pCh 23.1 was subcloned into the *Eco*RI site of pkOE and pMSGneo.

cDNA pCh 26.1 (2450 bp) (31) encodes the α4 ACh-binding subunit of chicken brain AChRs. By complete digestion with *Ava*I and partial digestion with *Dra*III, a fragment of pCh 26.1 was isolated containing 17 bp of 5′ untranslated region and 16 bp of 3′ untranslated region. The fragment was blunt ended with Klenow polymerase and T4 polymerase, *Eco*RI linkers were added, and the fragment was subcloned into the *Eco*RI site of pkOE and pMSGneo (Fig. 1).

Transfections and Selection of Cell Lines

Mouse Ltk⁻ cells (obtained from Dr. Pam Mellon, Salk Institute), maintained in DMEM containing 10% fetal calf serum, were transfected by calcium phosphate precipitation (32, 33). Dishes (10 cm, containing about 5×10^5 cells) were transfected with 10 μg of pKOneo and 1.7 μg each of pkOE-23.1 and pkOE-26.1 or with 10 μg each of pMSGneo-23.1 and pMSGneo-26.1. Transfected cells were cultivated for 3 days in normal culture medium, split 1:4, and grown for 1 week in medium containing 1 mg/ml Geneticin (GIBCO) and then for 3 weeks in medium containing 2 mg/ml Geneticin. Cells were subsequently maintained in culture medium containing 0.5 mg/ml Geneticin. Resistant cells were cloned by limiting dilution (0.5 cells/well of a 96-well tissue culture plate). Ten cell lines (pkOE-AChR 1–10 and pMSGneo-AChR 1–10) were obtained from each transfection and subsequently analyzed by Northern blotting and ligand binding.

For induction of expression of AChRs, pkOE-AChR cell lines were grown for 2–4 days in culture medium containing 10 mM sodium butyrate, and pMSGneo-AChR cell lines were grown for 3–4 days in culture medium containing 1 μM dexamethasone.

RNA Analysis

Cells were grown in 10-cm dishes and, when cells were almost confluent, sodium butyrate (10 mM final concentration) was added to pkOE cells and dexamethasone (1 μM final concentration) was added

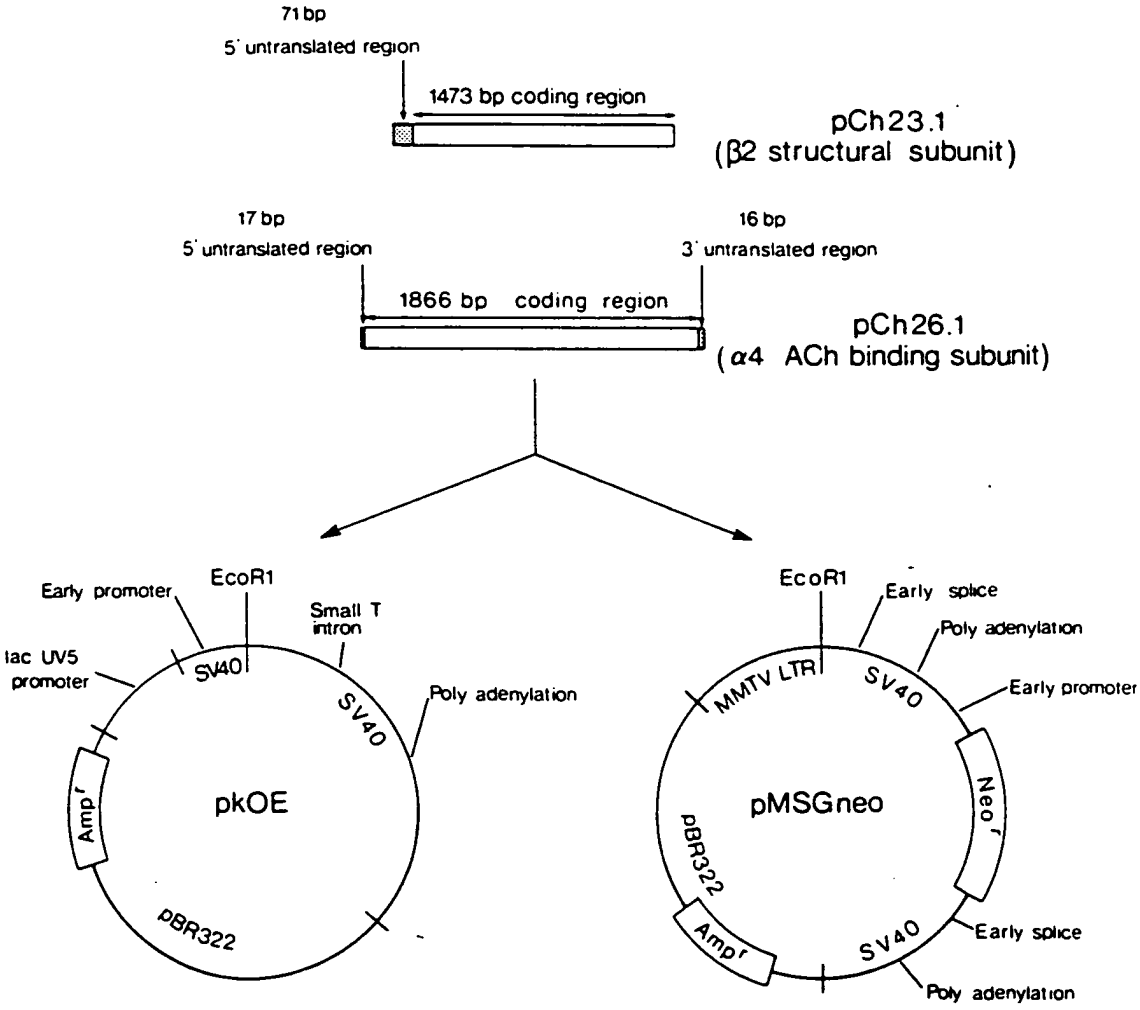

Fig. 1. Structure of vector constructs used for transfections.

to pMSGneo-AChR cells. After an additional 36 hr in culture, total cellular RNA was isolated according to the method of Gough (34). Half of the RNA from each cell line was analyzed by electrophoresis through a 1% agarose-formaldehyde gel and Northern blotting (35) onto Hybond-N (Amersham) membranes.

Hybridization of Northern blots was performed using random-primed ^{32}P-probes prepared from *Eco*RI inserts of pCh 23.1 and pCh 26.1 Hybridization was performed under high stringency in 5 × SSPE (1× SSPE is 0.18 M NaCl, 10 mM $NaPO_4$, pH 7.4, 1 mM EDTA), 50% formamide, at 42°. Filters were washed at 65° in 0.3 × SSPE and exposed to Kodak XAR film for 6 hr to 3 days, at −70°, using a Cronex QIII intensifying screen.

Preparation of Solubilized AChRs

Dishes (10 cm) or flasks (175 cm^2) were seeded with cell lines and grown until just confluent. Inducer (either sodium butyrate at a final concentration of 10 mM or dexamethasone at a final concentration of 1 μM) was added, and the cells were then generally grown for 3–4 days to allow expression of AChR. The cells were harvested by scraping into ice-cold 10 mM $NaPO_4$, pH 7.5, 100 mM NaCl (PBS), containing 10 mM EDTA, 10 mM EGTA, 5 mM iodoacetamide, and 1 mM PMSF, and were centrifuged (800 × *g*, 5 min) in a bench-top clinical centrifuge. The cell pellet was then solubilized in approximately 5–7.5 volumes of the aforementioned buffer, containing 0.5% Triton X-100, by agitation using a bench-top vortexer (small volumes) or by homogenization using a Semat Ultra-Turrax homogenizer (larger volumes). After gentle rotation for 30 min at 4°, particulate material was removed by centrifugation for 30 min at 4° in a bench-top microfuge or for 30 min at 4° at 80,000 × *g*, in a Beckman Ti 50.2 rotor. AChR was solubilized from chicken brains (obtained from Pel-Freez Biologicals) as previously described (8, 11, 36).

Ligand Binding

Ligand binding to AChRs solubilized from transfected cells was carried out using an immunoimmobilization assay, which has been described previously (36). Aliquots of detergent extract (150–500 μl, containing 15–50 fmol of L-[^{3}H]nicotine binding sites), in 1.5 ml microfuge tubes, were gently rotated overnight at 4° with 0.5 μl of mAb 290 (raised to rat brain AChRs and cross-reacting with chicken brain AChRs) (10) and 25 μl of a 1:1 slurry of goat anti-rat IgG coupled to Sepharose CL-4B. The Sepharose slurry was then centrifuged briefly (15–20 s) in a microfuge and washed with 1 ml of PBS, 0.5% Triton X-100, by resuspension and centrifugation as described above. The Sepharose was then resuspended in 100 μl of L-[^{3}H]nicotine (72 Ci/mmol; Amersham) in PBS, 0.5% Triton X-100, and was incubated for 15 min at room temperature. Free L-[^{3}H]nicotine was then removed by rapid washing at 4° with 3 × 1 ml of ice-cold PBS, 0.5% Triton X-100, with repeated centrifugation and resuspension of the Sepharose pellet. Bound L-[^{3}H]nicotine was then removed by addition of 150 μl of 2.5% SDS to the Sepharose pellet, incubation for 15 min, and then removal of the supernatant for scintillation counting. Nonspecific binding of L-[^{3}H]nicotine was determined by omission of the mAb from the incubation mixture and was subtracted from total binding to give specific binding. Nonspecific binding was always <150 dpm, whereas total binding was always >600 dpm, except where indicated. Saturation binding curves were obtained by incubating immunoimmobilized AChRs with various concentrations of L-[^{3}H]nicotine. Inhibition of L-[^{3}H]nicotine binding to AChRs by cholinergic ligands was determined by including various concentrations of the ligands in the presence of 3 nM L-[^{3}H]nicotine. Except where stated, all points on binding curves were derived from triplicate tubes. K_i values were determined from three or four independent experiments and were calculated using the equation $K_i = IC_{50}/1 + [L\text{-}[^3H]\text{nicotine}]/K_d$. Ligand binding to AChRs solubilized from chicken brain was carried out as described above, except that AChRs were immobilized upon mAb 299 (raised to rat brain AChRs and directed to the α4 subunit, cross-reacting with chicken brain AChRs) (10).

Sucrose Gradient Sedimentation Analysis of AChRs

Sucrose gradient sedimentation analysis of AChRs was performed as previously described (8). Briefly, 100 μl of M10 cell detergent extract, to which purified *Torpedo* AChR (the gift of Dr. A. Vincent, Institute for Molecular Medicine, Oxford) was added (approximately 50 nM final concentration) as an internal standard, were layered onto 4.9-ml sucrose gradients (5–20%, w/w, in PBS, 0.5% Triton X-100) and centrifuged for 70 min at 4° at 65,000 rpm, in a Beckman vTi 65.2 rotor. Fractions (14 drops) were collected through a 19-gauge needle. Aliquots (20 μl) of each fraction were assayed for *Torpedo* AChR: 20 μl of PBS, 0.5% Triton X-100, containing ^{125}I-labeled α-bungarotoxin (the gift of Dr. A. Vincent), 0.5 μl of mAb 35 (which binds to *Torpedo* AChR) (37), and 25 μl of goat anti-rat IgG-Sepharose were added to each 20-μl aliquot. After gentle rotation overnight at 4°, the Sepharose beads were washed with 3 × 1 ml of PBS, 0.5% Triton X-100, and the ^{125}I-α-bungarotoxin bound to the immunoimmobilized *Torpedo* AChRs was quantitated by γ counting. Neuronal nicotinic AChRs in each fraction were quantitated by L-[^{3}H]nicotine binding using mAb 290 (which does not bind to *Torpedo* AChRs) (10), as described above.

Purification and SDS-PAGE of [^{35}S]methionine-labeled AChRs

[^{35}S]Methionine labeling of cells and immunoaffinity purification. A confluent 10-cm dish of M10 cells was induced for 16 hr with 1 μM dexamethasone, washed with 3 × 10 ml of methionine-free DMEM, and incubated for 6 hr at 37° in 2 ml of methionine-free DMEM containing 500 μCi of [^{35}S]methionine (71,000 Ci/mmol; Amersham). The cells were scraped off in 1 ml of PBS, pelleted, and then resuspended in 500 μl of lysis buffer (50 mM Tris, pH 7.5, 200 mM NaF, 1% Triton X-100, 5 mM EDTA, 5 mM EGTA, 5 mM iodoacetamide, 1 mM PMSF) containing 5 mg/ml bovine serum albumin (from a 50 mg/ml stock in 1% SDS), 10 μg/ml leupeptin, 10 μg/ml pepstatin, and 10 μg/ml antipain. After 15 min of gentle rotation at 4°, insoluble material was removed by centrifugation for 30 min at 4° in a microfuge. The extract was preabsorbed by gentle rotation at 4° for 15 min with 50 μl of goat anti-rat IgG coupled to Sepharose. This was removed by centrifugation, and the extract was then gently rotated for 4 hr at 4° with 25 μl of mAb 295 coupled to AFC resin (New Brunswick Sceintific) (10). The cell extract was then removed by centrifugation, and the resin was washed with 5 × 1 ml of lysis buffer, 5 × 1 ml of lysis buffer containing 800 mM NaCl, and 2 × 1 ml of lysis buffer, by repeated centrifugation and resuspension. AChRs were then eluted by incubation of the resin for 2 × 10 min in 50 μl of 50 mM citrate, pH 3.0, containing 0.01% Triton X-100, and 2 min in 100 μl of H_2O. The eluate was neutralized with 1 M Tris, pH 7.5, concentrated using a Centricon (Amicon) to approximately 50 μl, diluted with 1 ml of H_2O, concentrated, and then lyophilized.

Glycopeptidase F treatment and SDS-PAGE analysis. Lyophilized immunoaffinity-purified AChRs were resuspended in H_2O, and a 10-μl aliquot was adjusted to contain 0.75% SDS and 1.5% β-mercaptoethanol and was then heated to 90° for 3 min. Buffer (35 μl of 10 mM $NaPO_4$, pH 7.5, 0.75% Triton X-100, 5 mM EDTA, 5 mM EGTA, 1 mM PMSF, 10 μg/ml leupeptin, pepstatin, and antipain, containing 2.5 units of glycopeptidase F; Boehringer) was added, followed by incubation overnight at 37°. The AChR was then analyzed by SDS-9% PAGE and fluorography, using prestained protein standards for apparent molecular weight determination.

Electrophysiological Recordings

For electrophysiological recordings, M10 cells were subcultured onto uncoated glass coverslips. Coverslips were transferred to a glass-bottomed Perspex recording chamber mounted on the stage of a Nikon Diaphot inverted microscope. Cultures were observed using phase contrast optics and were continuously perfused (approximately 1 ml/min) with a salt solution of the following composition (in mM): NaCl, 124; KCl, 3.25; $MgCl_2$, 2; $CaCl_2$, 2; HEPES, 10; D-glucose, 11; pH 7.4 using NaOH. In a number of experiments, cell cultures were briefly treated

with trypsin/EDTA solution (GIBCO) before transfer to the recording chamber. This had the effect of changing the M10 cell morphology from the usual flat sheet-like appearance to a more rounded form and facilitated both seal formation and viability. The enzyme treatment had no discernable effect on agonist-evoked nicotinic responses.

Patch pipettes with an approximate tip diameter of 1 μm were pulled from boroscilicate glass (Clark Electromedical) using a Mechanex BBCH puller. No additional fire-polishing was performed, and pipettes had a resistance of 5.8 ± 1 MΩ (mean ± standard error; $n = 5$) when filled with the following solution (in mM): CsF, 120; CsCl, 10; HEPES, 10; EGTA, 10; $CaCl_2$, 0.0005; pH adjusted to 7.3 with CsOH.

Whole-cell currents were recorded from voltage-clamped M10 cells using a LIST EPC-7 amplifier, 3–5 days after plating and induction with 1 μM dexamethasone. After formation of a high resistance seal with the cell under investigation, capacitance transients were minimized using the C-Fast facility on the EPC-7. Mean seal resistance measured from five cells was 5.7 ± 0.8 GΩ. No additional capacitance compensation was applied, and no compensation was made for series resistance. All experiments were performed at a holding potential of −75 mV, unless otherwise indicated.

Drugs were applied by gravity perfusion from a large bore (approximately 100 μm) double-barrelled pipette assembly positioned 100–150 μm from the cell. The pipette assembly was positioned using a motorized micromanipulator. Fast on-off drug applications were made by stepping the arrangement laterally such that the cell under investigation experienced a rapid change from control solution flowing from one of the barrels to drug solution flowing from the adjacent barrel.

Results

Preparation of expression system. To allow expression of a multisubunit protein such as a neuronal nicotinic AChR in transfected cells, both stable integration and subsequent expression of cDNAs encoding the AChR must be achieved. Two different mammalian expression systems were used, one utilizing a SV40 promoter (pkOE vector) and the other utilizing the dexamethasone-inducible MMTV promoter (pMSGneo vector) (Fig. 1). An expression vector with an inducible promoter was used to circumvent the possibility that constitutive expression of neuronal AChRs with functional ion channels may be in some way toxic to the transfected cell.

The cDNAs encoding the β2 structural subunit (pCh 23.1) and the α4 ACh-binding subunit (pCh 26.1) were engineered to remove the majority of the untranslated regions (Fig. 1). As such, the expression of these cDNAs should be totally under the control of the transcription signals present in the expression vector.

Mouse fibroblast L cells were co-transfected with either pMSGneo-Ch 23.1 and pMSGneo-Ch 26.1 or pkOE-Ch 23.1, pkOE-Ch26.1, and pkOE-neo (Fig. 1). Cells were selected for neomycin resistance, and resistant cells were subcloned by limiting dilution. Clonal cell lines were subsequently analyzed for expression of subunit mRNAs and expression of L-[^{3}H] nicotine binding sites.

RNA analysis of transfected cell lines. Ten stable cell lines transfected with either pkOE vectors (pkOE-AChR 1–10) or pMSGneo vectors (pMSGneo-AChR 10–10) were obtained. Cell lines pMSGneo-AChR 1–3 were subsequently lost. Each clonal cell line was analyzed for expression of AChR subunit mRNAs. To induce the transcription of RNAs driven by the SV40 promoter of pkOE-AChR-transfected cells, cultures were grown for 36 hr in the presence of 10 mM sodium butyrate, which is known to increase expression of transcription from the SV40 early promoter (38). To induce transcription of RNAs driven by the MMTV promoter of pMSGneo-AChR-transfected cells, cultures were grown for 36 hr in the presence of 1 μM dexamethasone. RNA was isolated and subjected to Northern blot analysis (Fig. 2). Less than half of the cell lines expressed detectable amounts of subunit RNAs. With the exception of the expression of pCh23.1 RNA in pkOE-AChR 7, a single species of RNA was expressed, which was considerably larger than the size of the cDNAs (Fig. 1), indicating addition of other sequences and probably a poly(A) tail.

Expression of L-[^{3}H]nicotine binding sites. To determine which cell lines expressed assembled AChRs capable of binding ligand, a confluent 10-cm dish of each cell line was cultured for 3 days in the presence of the appropriate inducer (either 10 mM sodium butyrate or 1 μM dexamethasone), the cells were harvested and solubilized, and L-[^{3}H]nicotine binding was determined by an immunoimmobilization assay, as described in Materials and Methods. mAb 290 was used in all the binding assays described below. This mAb is directed to the β2 structural subunit encoded by cDNA pCh 23.1 but binds only to native AChRs, having little or no affinity for denatured

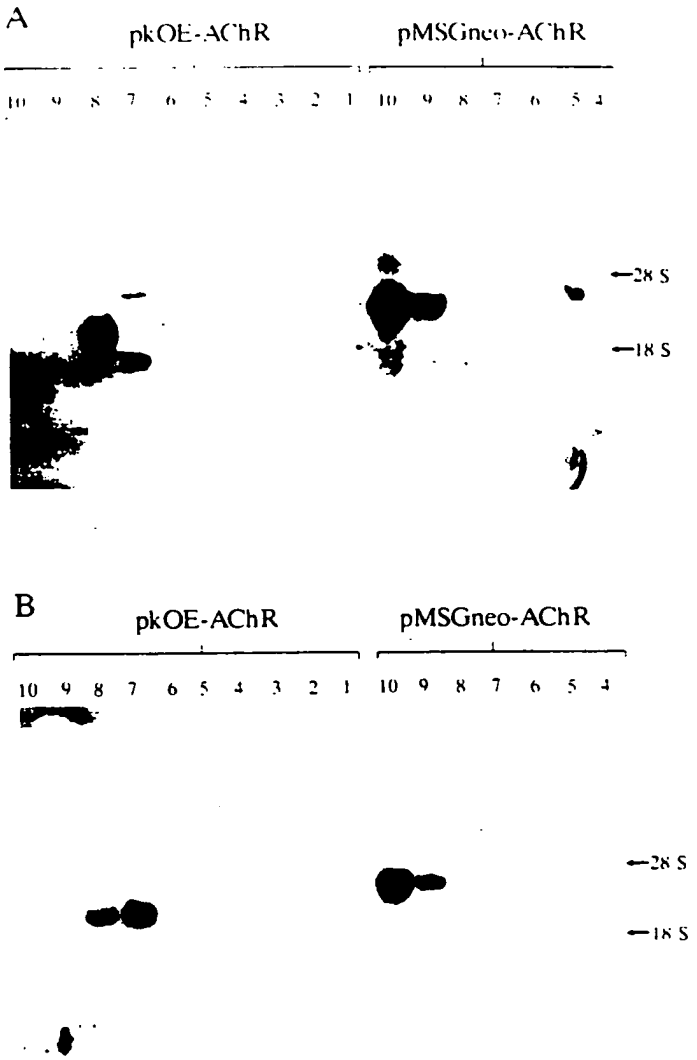

Fig. 2. Northern blot analysis of transfected cell lines. RNA from transfected cell lines (pMSGneo-AChR 4–10 and pkOE-AChR 1–10) was analyzed as described in Materials and Methods. Blots were hybridized under high stringency conditions with random-primed ^{32}P-probes prepared from the *Eco*RI inserts of pCH 23.1 (A) and pCh 26.1 (B).

subunits (10). We have obtained similar results using other mAbs directed to $\beta 2$ (mAbs 270 and 295) and to $\alpha 4$ (mAbs 286 and 299). Only two cell lines, pkOE-AChR 8 (P8) and pMSGneo-AChR 10 (M10), expressed L-[^{3}H]nicotine binding sites significantly above background nonspecific binding (data not shown).

The time course of expression of AChRs by P8 and M10 cells was then determined (Fig. 3). Uninduced cells had no detectable L-[^{3}H]nicotine binding sites. After addition of 1 μM dexamethasone to M10 cells, there was a relatively rapid induction of AChR expression, as measured by L-[^{3}H]nicotine binding sites, reaching maximal levels of about 30,000 dpm (190 fmol) of L-[^{3}H]nicotine binding sites/10-cm culture dish by 48–72 hr. After addition of 10 mM sodium butyrate to P8 cells, there was a somewhat slower induction of AChRs, reaching maximal levels of about 3000 dpm (19 fmol) of L-[^{3}H]nicotine binding sites/10-cm culture dish by 80–120 hr. Thus, approximately 10-fold higher expression of AChRs by M10 cells was found, compared with P8 cells, reaching levels of 10,700 AChR molecules/cell (mean of three determinations), assuming two L-[^{3}H]nicotine binding sites/AChR molecule. Similar levels of expression have been reported for L cells transfected with *Torpedo* AChRs (4). The specific activity of detergent extracts of pMSGneo-AChR 10 cells was 0.4–0.5 pmol/mg of protein. This is approximately 16-fold higher than the specific activity of AChRs in detergent extracts of chicken brains (about 0.028 pmol mg of protein) (8). Subsequent studies thus focused upon M10. This cell line has been maintained in continuous culture for time periods of up to 5 months, and has been retrieved from frozen storage, without any obvious loss of ability to express AChRs.

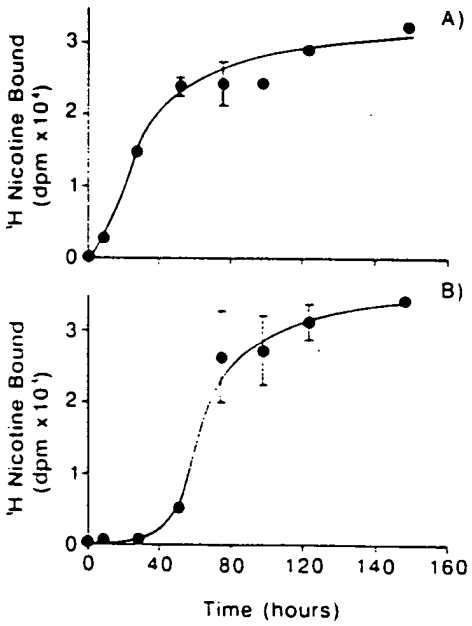

Fig. 3. Time course of induction of AChR expression in M10 cells (A) and P8 cells (B). Transfected cell lines were seeded into 10-cm tissue culture dishes and, when cells were semiconfluent (time zero), fresh culture medium containing 1 μM dexamethasone (A) or 10 mM sodium butyrate (B) was added to the dishes. At various time intervals thereafter, cells were harvested by washing the monolayer in 10 ml of PBS, scraping off the cells in 10 ml of PBS, pelleting, and freezing the cell pellet. When the cells at each time point had been harvested, the cell pellets were solubilized in 500 μl of PBS containing 0.5% Triton X-100, 10 mM EDTA, 10 mM EGTA, 5 mM iodoacetamide, and 1 mM PMSF, and L-[^{3}H]nicotine binding was determined as described in Materials and Methods. Each data point (shown as mean ± standard deviation) is the mean of values determined from three tissue culture dishes, except for the 122-hr and 144-hr time points, where two tissue culture dishes were used. L-[^{3}H] Nicotine binding sites are expressed as dpm/tissue culture dish.

Pharmacological characterization of recombinant and native $\alpha 4\beta 2$ AChRs. Radioligand binding studies were performed using AChRs solubilized with Triton X-100 detergent, from either M10 cells or chicken brains and then immobilized upon a mAb, as described above. AChRs from chicken brain were immobilized upon mAb 299 (10). This mAb is directed to the $\alpha 4$ subunit and only binds the $\alpha 4\beta 2$ AChR subtype from chicken brain, thus allowing direct comparison of the pharmacology of the native AChR with that of the $\alpha 4\beta 2$ AChR expressed by M10 cells. L-[^{3}H]Nicotine binding to the immunoimmobilized M10 AChRs was both saturable and of high affinity ($K_d = 3.2 \pm 1 \times 10^{-9}$ M; mean ± standard deviation of four determinations) (Fig. 4). An almost identical value was obtained for L-nicotine binding to $\alpha 4\beta 2$ AChRs from chicken brain ($K_d = 3.6 \pm 0.3 \times 10^{-9}$ M; mean ± standard deviation of three determinations; data not shown). The L-[^{3}H]nicotine binding to both AChRs from M10 cells and AChRs from chicken brain was displaced by competing cholinergic agonists and antagonists, with very similar K_i values (Table 1). The correlation of these values was excellent (Fig. 5), with a correlation coefficient of 0.998. These K_i values are also in good agreement with values determined for AChRs from rat brain (39–41).

Structure of AChRs expressed by M10 cells. Both the macromolecular size and the subunit structure of AChRs expressed by M10 were determined. The macromolecular size was analyzed by sucrose gradient sedimentation analysis of detergent-solubilized AChRs. As previously described (8, 10), *Torpedo* AChR was used as an internal size marker, sedimenting at 9 S (monomer) and 13 S (dimer) (42). By resolving *Torpedo* AChR on the same gradient as the transfected cell detergent extract, any possible variation between gradients was eliminated. AChRs from the transfected cells reproducibly sedimented as a single peak, which ran slightly ahead (about 10 S) of *Torpedo* AChR monomers (Fig. 6). Thus, the expressed AChR behaves the same as native brain AChRs upon sucrose gradient analysis (8–10). The subunit structure of the recombinant AChRs was defined by [^{35}S]methionine labeling of M10 cells and immunoaffinity purification of radiolabeled AChRs using mAb295. Like mAb290, mAb295 binds to native AChRs, showing little binding to denatured subunits (10). Thus, it probably binds with highest affinity to receptor macromolecules that have been correctly assembled to achieve a native conformation. SDS-PAGE and autoradiography of recombinant AChRs revealed two closely migrating doublets of apparent M_r 50,000 and 75,000 (Fig. 7). This corresponds to the expected size of the $\beta 2$ and $\alpha 4$ subunits, respectively (11). By excising the part of the polyacrylamide gel corresponding to the $\alpha 4$ and $\beta 2$ subunit bands, quantitating the radioactivity in each band by scintillation counting, and normalizing the radioactivity for the number of methionine residues in each subunit (see Ref. 26 for details), a subunit stoichiometry of 2:3.55 ± 0.22 (mean ± standard deviation of two determinations) $\alpha 4{:}\beta 2$ was found. This value is in reasonable agreement with a stoichiometry of $(\alpha 4)_2(\beta 2)_3$ previously obtained in more detailed studies of AChRs expressed in *Xenopus* oocytes, using either metabolic labeling techniques (26), as above, or an electrophysiological approach (27).

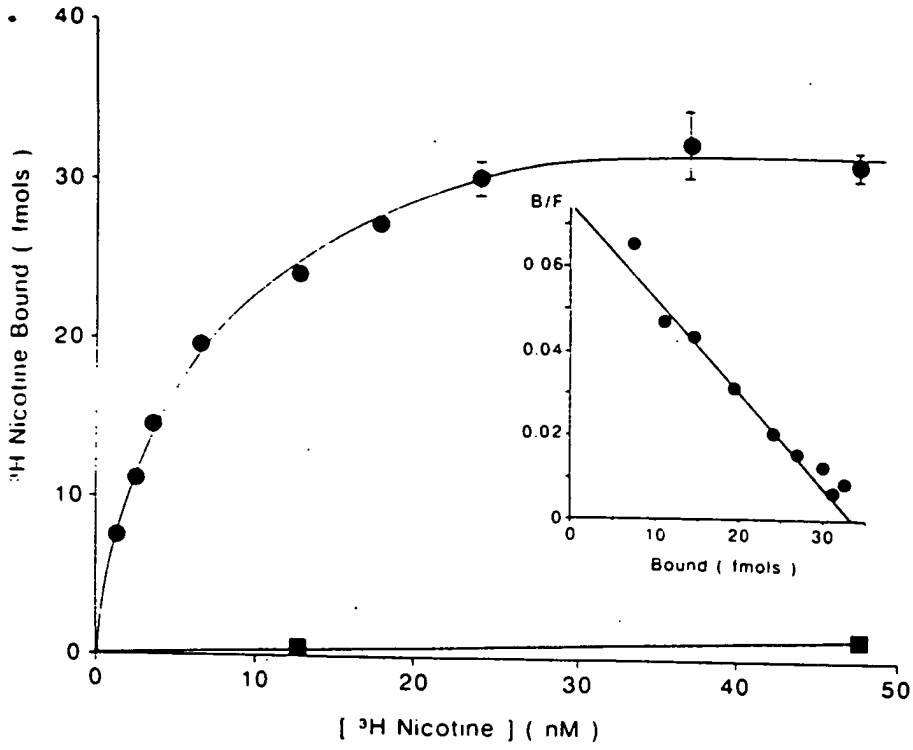

Fig. 4. Binding of L-[³H]nicotine to immunoimmobilized AChRs solubilized from M10 cells. Binding assays were performed exactly as described in Materials and Methods. Each point is the mean ± standard deviation of three values. ●, Specific binding; ■, nonspecific binding, determined by omission of mAb 290. *Inset*, Scatchard analysis of the data, displayed as bound/free (*B/F*) (fmol/fmol) versus bound (fmol).

TABLE 1

Inhibition by cholinergic ligands of L-[³H]nicotine binding to AChRs solubilized from transfected cells and chicken brains

K, values are the mean ± standard deviation of three or four determinations.

Competing ligand	*K*,	
	α4β2 AChR from transfected cells	α4β2 AChR from chicken brain
	M	
Cytisine	$1.4 \pm 0.3 \times 10^{-10}$	$1.4 \pm 0.4 \times 10^{-10}$
L-Nicotine	$3.9 \pm 2.1 \times 10^{-9}$	$2.4 \pm 0.5 \times 10^{-9}$
Carbachol	$3.6 \pm 1.3 \times 10^{-7}$	$4.5 \pm 1.2 \times 10^{-7}$
D-Tubocurarine	$2.5 \pm 1.4 \times 10^{-5}$	$7.7 \pm 1.5 \times 10^{-6}$
Hexamethonium	$3.0 \pm 0.6 \times 10^{-4}$	$1.6 \pm 0.5 \times 10^{-4}$
Mecamylamine	$>10^{-3}$	$>10^{-3}$

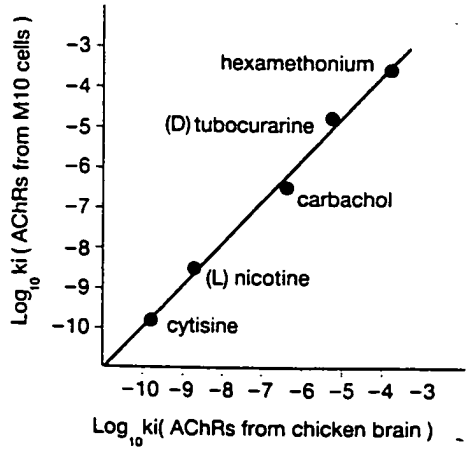

Fig. 5. Correlation between the affinities for nicotinic cholinergic ligands of α4β2 AChRs expressed by M10 cells and α4β2 AChRs from chicken brain.

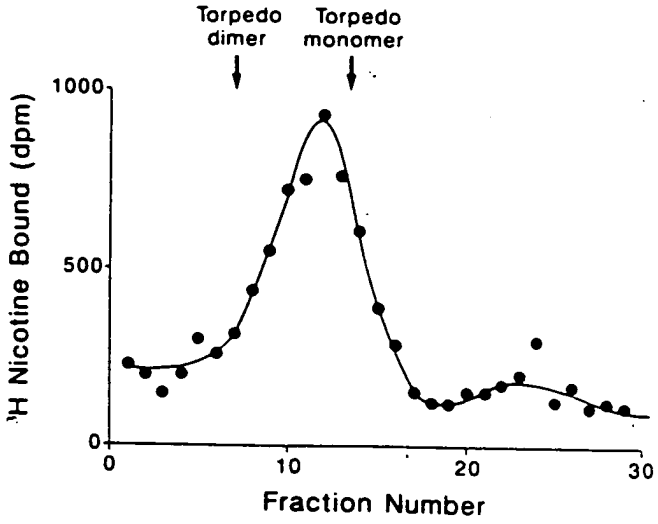

Fig. 6. Sucrose gradient sedimentation analysis of AChRs expressed in M10 cells. *Arrows*, positions of *Torpedo* AChR monomer (9 S) and dimer (13 S), which were resolved on the same gradient, as internal standards.

The polypeptide doublets observed for [³⁵S]methionine-labeled AChRs probably result from differences in processing of carbohydrate groups. This was confirmed by treatment of purified AChRs with glycopeptidase F; the doublets were resolved to single deglycosylated polypeptides, of apparent M_r 43,000 and 64,000. The deduced molecular weights of β2 and α4 are 54,000 and 68,400, respectively (15, 18, 31), somewhat larger than the apparent molecular weight of the deglycosylated polypeptides. This discrepancy between apparent and deduced molecular weight has been reported for other polypeptides; for instance, *Torpedo* electric organ AChR α subunits have an apparent molecular weight of 40,000 (2) but a deduced molecular weight of 50,116 (43).

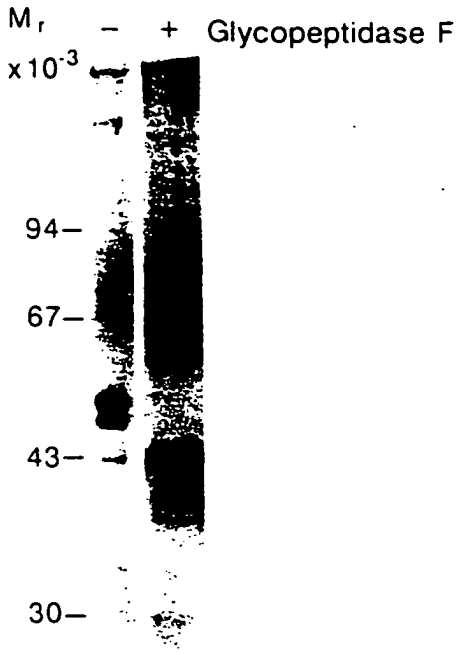

Fig. 7. Subunit structure of AChRs expressed by M10 cells. AChRs were immunoaffinity purified from [^{35}S]methionine-labeled cells and then analyzed by SDS-9% PAGE and fluorography. AChRs that had been treated with glycopeptidase F are also shown. The positions of prestained molecular weight standards are shown to the *left*.

Expression of ACh-gated ion channels. The electrophysiological effects of ACh were studied on approximately 50 M10 cells in which the expression of the AChR had been induced by the addition of dexamethasone (1 μM) to the culture medium for 3–5 days. In all cases, ACh evoked an inward current at negative pipette potentials. ACh responses were not observed in cells that had not been induced by dexamethasone. Muscarine (100 μM) failed to elicit a response in induced cells (n = 3), and responses to ACh were not modified by the addition of atropine (1 μM) to the perfusate, confirming that the responses were not due to endogenous muscarinic AChRs.

Brief applications (0.5–1 sec) of either ACh (30 μM) or the selective nicotonic agonist DMPP (30 nM) (data not shown) characteristically evoked responses that were rapid in onset but desensitized in the presence of the agonist (Fig. 8). Responses to ACh were antagonized by hexamethonium, D-tubocurarine, and DHβE (Fig. 8). The effects of hexamethonium (0.1–10 μM) were studied on six cells. In all cases, the responses to ACh were reduced and were not readily reversible, despite extensive washing. D-Tubocurarine (10 μM) reduced the response to ACh (30 μM) to 34 ± 2% (mean ± standard error; n = 4) of control. DHβE, at concentrations of 300 nM, significantly antagonized the responses to ACh, indicating that DHβE is a potent antagonist at these AChRs.

The amplitude of the current response to ACh was found to be dependent not only on the agonist concentration but also on the pipette potential. The current-voltage (I-V) relationship was studied more fully on five cells. The ACh response consistently showed a marked inward rectification, such that outward membrane currents at positive pipette potentials were not apparent (Fig. 9). The inward current response was approximately linear over the pipette potential range of −50 to −100 mV and, when measured over this range, current amplitude was found to change e-fold (2.718) with a mean 5.5 ± 1.3-mV (n = 5) change in potential.

Discussion

Here we have reported the stable expression in mouse fibroblasts of a neuronal nicotinic AChR composed of α4 and β2 subunits. Initially, two systems of expression vectors were explored, an SV40 promoter-driven system and an MMTV promoter-driven system. In what should be considered to be a very limited comparison, the latter system appeared more suitable, giving more rapid induction of expression and significantly higher levels of expression. In the absence of the inducer, expression of AChRs was below detectable levels (Fig. 4). Overall, we found that only a small proportion of transfected cell lines (2 of 17) expressed detectable amounts of AChR.

The macromolecular size and the subunit structure of AChRs expressed by M10 cells were indistinguishable from those of native brain α4β2 AChRs. Sucrose gradient sedimentation analysis (Fig. 6) demonstrated that, like native brain AChRs, recombinant α4β2 AChRs sediment as a 10 S species (8, 10). [^{35}S]Methionine labeling and immunoaffinity purification using a subunit-specific mAb demonstrated that these recombinant AChRs are formed by coassembly of β2 and α4 subunits. Previous studies using oocytes have assumed that this occurs (21–24). The apparent molecular weights of the subunits were essentially identical to those of α4β2 AChRs purified from chicken brain (11). Because recombinant AChR subunits were very similar in size to subunits of AChRs purified from brain, the glycosylation performed by the transfected cell must be almost equivalent to that performed normally by a neuron. The doublets observed upon SDS-PAGE analysis of recombinant AChRs represent incomplete processing of the added carbohydrate moieties (Fig. 7). It remains to be determined whether this incompletely glycosylated form of the subunits is present in the native AChR expressed on the cell surface or whether it is a glycosylation intermediate found in the Golgi apparatus that we have been able to visualize by virtue of the very rapid rate of subunit synthesis achieved at 20 hr after induction (Fig. 3). Quantitation of the [^{35}S]methionine incorporated into the AChR subunits allowed determination of a subunit stoichiometry for α4:β2 of 2:3.5. In a more detailed investigation of stoichiometry, using the same approach for AChRs expressed in *Xenopus* oocytes, we have determined the subunit arrangement to be a pentamer of $(\alpha4)_2(\beta2)_3$ (26). The reasonable agreement between these two values indicates that the subunit stoichiometry is independent of the expression system.

Pharmacological analysis indicated that the ligand-binding properties of α4β2 AChRs expressed by M10 cells and native α4β2 AChRs from chicken brain were approximately identical. Clearly, the very similar macromolecular size and pharmacological profile of these recombinant α4β2 AChRs, compared with those of the major AChR subtype solubilized from brain, which has been proposed to consist of α4 and β2 subunits (9, 11, 18), is very strong evidence that this subunit composition is correct.

The ability of ACh to evoke membrane current responses in M10 cells that had been induced by dexamethasone, but not in uninduced cells, indicates that the binding sites labeled by L-[^{3}H]nicotine constitute AChRs with functional ion channels. The responses to ACh were blocked by hexamethonium, D-tubocurarine, and DHβE, confirming the nicotinic cholinergic

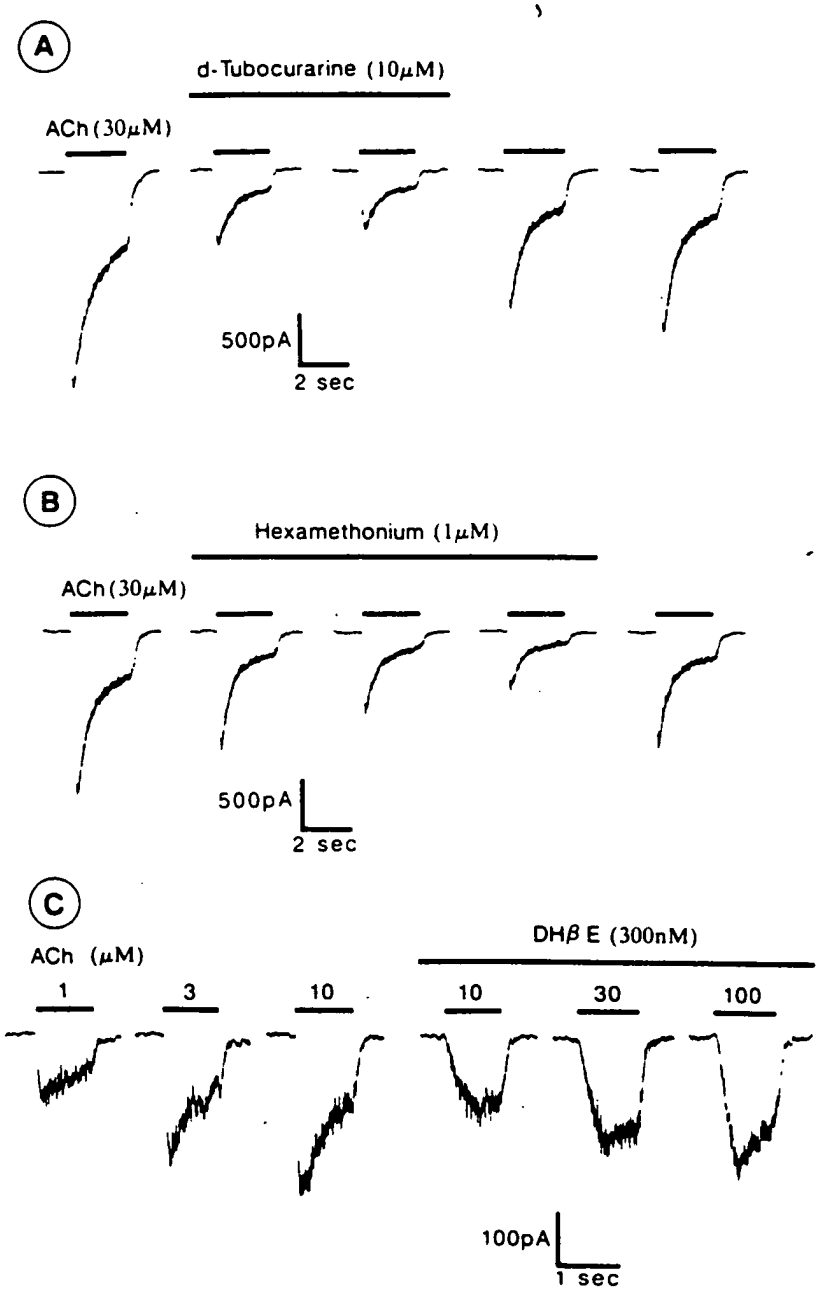

Fig. 8. Membrane current responses induced by ACh are antagonized by D-tubocurarine, hexamethonium, and DHβE. A and B, responses to 2 sec applications of ACh were obtained at approximately 30-sec intervals, using the fast perfusion system described in Materials and Methods. After stable control ACh responses were obtained, either D-tubocurarine (10 μM) (A), hexamethonium (1 μM) (B), or DHβE (C) was applied. D-Tubocurarine produced a rapid antagonism, which was readily reversible. Hexamethonium provided a more slowly developing block, which appeared to be use dependent and was often only poorly reversible. The final response in B was obtained after washing of the cell in antagonist-free solution for approximately 2 min. C, Inward currents were elicited in response to increasing concentrations of ACh. The cell was then continuously perfused with DHβE (300 nM); higher concentrations of ACh were required to evoke similar inward currents in the presence of the antagonist. Note the slower on-rate kinetics of the ACh response in the presence of DHβE; this is most likely to be the consequence of a slow rate of dissociation of the antagonist from the receptor during the approach to equilibrium. Cells were voltage clamped at −75 mV.

nature of the response. In the future, a more detailed and extensive study will define the electrophysiological properties of these $\alpha4\beta2$ AChRs. A significant characteristic of the functional response we did observe was a strong inward rectification. The phenomenon has been observed in whole-cell recordings of nicotinic AChRs in neurons dissociated from rat sympathetic ganglia (44) and in cultured PC12 pheochromocytoma cells (45). Thus, inward rectification may be a common property of neuronal AChR subtypes. Its physiological role, however, remains open to speculation.

We have previously proposed that the major subtype of nicotinic AChRs in the brain is composed of two types of subunits, structural (encoded by cDNA $\beta2$) and ACh-binding (encoded by cDNA $\alpha4$) (18, 25). The expression of functional ACh-gated cation channels composed of $\alpha4$ and $\beta2$ subunits in oocytes (21–24) and mouse fibroblasts (Fig. 8) supports this hypothesis, as does the essentially identical pharmacology and structure of recombinant $\alpha4\beta2$ AChRs expressed in fibroblasts, compared with those of native AChRs (Table 1). However, it is still possible that some subpopulations of $\alpha4\beta2$ AChRs in the brain do contain an additional subunit that has eluded detection. A role for the putative structural subunits $\beta3$ and $\beta4$ has yet to be determined. They certainly appear to be of lower abundance and more limited distribution than $\beta2$ and $\alpha4$ (19, 20). It is possible that in certain regions of the brain they may associate with an α subunit in addition to, or in place of, $\beta2$.

We have shown here, by synthesis in a stably transfected cell line, that AChRs with the subunit composition $\alpha4\beta2$, determined initially by analysis of AChRs purified from brain, in fact exhibit the properties expected of the predominant brain AChR subtype *in vivo*. Such stable cell lines may provide a useful system for study of the function and pharmacology of a

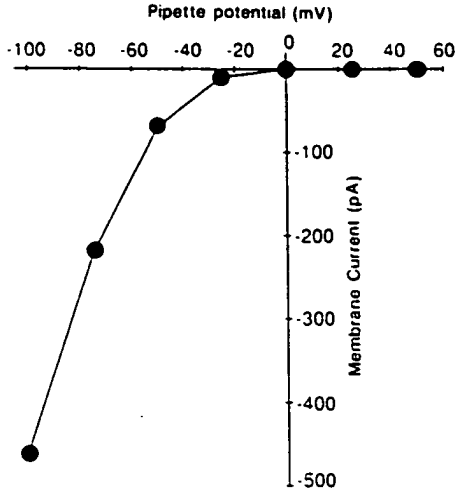

Fig. 9. Current-voltage relationship for ACh-evoked whole-cell currents. The amplitude of the membrane current evoked by brief applications of ACh (30 μM) is plotted as a function of pipette potential. M10 cells characteristically showed strong inward current rectification. Outward currents at positive pipette potentials were not observed. Inward currents increased in amplitude with membrane hyperpolarization, with the relationship being approximately linear over the range of −50 to −100 mV.

single AChR subtype of known subunit composition. Future studies will attempt to utilize this expression system for more detailed study of AChR subunit topology, assembly, function, and regulation.

Acknowledgments

We would like to thank Dr. Angela Vincent, Institute of Molecular Medicine (Oxford) for providing *Torpedo* AChR and ^{125}I-α-bungarotoxin. We would like to thank Drs. Ian Ragan, John Kemp, and Les Iversen for support of this work.

References

1. Unwin, N. The structure of ion channels in membranes of excitable cells. *Neuron* 3:665–676 (1989).
2. Changeux, J. P. Functional architecture and dynamics of the nicotinic acetylcholine receptor: an allosteric ligand gated ion channel. *Fidia Research Foundation Neuroscience Award Lectures* (J. P. Changeux, R. Llines, D. Purves, and F. Bloom, eds.), Vol. 4. Raven Press, New York, 21–168 (1990).
3. Mishina, M., T. Tobimatsu, K. Imoto, K. Tanaka, Y. Fujita, K. Fukuda, M. Kurasaki, H. Takahashi, Y. Morimoto, T. Hirose, S. Inayama, T. Takahashi, M. Kuno, and S. Numa. Localization of functional regions of acetylcholine receptor α subunit by site directed mutagenesis. *Nature (Lond.)* 313:364–369 (1985).
4. Claudio, T., W. N. Green, D. S. Hartman, D. Hayden, H. L. Paulson, F. J. Sigworth, S. M. Sine, and A. Swedlund. Genetic reconstitution of functional acetylcholine receptor channels in mouse fibroblasts. *Science (Washington D. C.)* 238:1688–1694 (1987).
5. Forsyth, J., A. Franco, A. Rossi, J. Lansman, and Z. Hall. Expression of functional mouse muscle acetylcholine receptors in Chinese hamster ovary cells. *J. Neurosci.* 10:2771–2779 (1990).
6. Blount, P., M. Smith, and J. P. Merlie. Assembly intermediates of the mouse muscle nicotinic acetylcholine receptor in stably transfected fibroblasts. *J. Cell. Biol.* 111:2601–2611 (1990).
7. Saedi, M., W. Conroy, and J. Lindstrom. Assembly of *Torpedo* acetylcholine receptor in *Xenopus* oocytes. *J. Cell. Biol.* 112:1007–1015 (1991).
8. Whiting, P. J., and J. M. Lindstrom. Purification and characterization of a nicotinic acetylcholine receptor from chick brain. *Biochemistry* 25:2082–2093 (1986).
9. Whiting, P. J., and J. M. Lindstrom. Purification and characterization of a nicotinic acetylcholine receptor from rat brain. *Proc. Natl. Acad. Sci. USA* 84:595–599 (1987).
10. Whiting, P. J., and J. M. Lindstrom. Characterization of bovine and human neuronal nicotinic acetylcholine receptors using monoclonal antibodies. *J. Neurosci.* 8:3395–3404 (1988).
11. Whiting, P. J., R. Liu, B. J. Morley, and J. M. Lindstrom. Structurally different neuronal nicotinic acetylcholine receptor subtypes purified and characterized using monoclonal antibodies. *J. Neurosci.* 7:405–416 (1987).
12. Boulter, J., K. Evans, D. Goldman, G. Martin, D. Treco, S. Heinemann, and J. Patrick. Isolation of a cDNA clone coding for a possible neuronal nicotinic acetylcholine receptor *alpha* subunit. *Nature (Lond.)* 319:368–374 (1986).
13. Goldman, D., E. Deneris, W. Luyten, A. Kochhar, J. Patrick, and S. Heinemann. Members of a nicotinic acetylcholine receptor gene family are expressed in different regions of the mammalian central nervous system. *Cell* 48:965–973 (1987).
14. Wada, K., M. Ballivet, J. Boulter, J. Connolly, E. Wada, E. S. Deneris, L. W. Swanson, S. Heinemann, and J. Patrick. Functional expression of a new pharmacological subtype of brain nicotinic acetylcholine receptor. *Science (Washington D. C.)* 240:330–334 (1988).
15. Nef, P., C. Oneyser, C. Alliod, S. Couturier, and M. Ballivet. Genes expressed in the brain define three distinct neuronal acetylcholine receptors. *EMBO J.* 7:595–601 (1988).
16. Boulter, J., A. O'Shea-Greenfield, R. M. Duvoisin, J. G. Connolly, E. Wada, A. Jensen, P. D. Gardner, M. Ballivet, E. S. Deneris, D. McKinnon, S. Heinemann, and J. Patrick. α2, α5 and β4: three members of the rat neuronal nicotinic acetylcholine receptor-related gene family form a gene cluster. *J. Biol. Chem.* 265:4472–4482 (1990).
17. Deneris, E. S., J. Connolly, J. Boulter, E. Wada, K. Wada, L. W. Swanson, J. Patrick, and S. Heinemann. Primary structure and expression of β2: a novel subunit of neuronal nicotinic acetylcholine receptors. *Neuron* 1:45–54 (1988).
18. Schoepfer, R., P. Whiting, F. Esch, R. Blacher, S. Shimasaki, and J. Lindstrom. cDNA clones coding for the structural subunit of a chicken brain nicotinic acetylcholine receptor. *Neuron* 1:241–248 (1988).
19. Deneris, E. S., J. Boulter, L. W. Swanson, J. Patrick, and S. Heinemann. β3: a new member of nicotinic acetylcholine receptor gene family is expressed in brain. *J. Biol. Chem.* 264:6268–6272 (1989).
20. Duvoisin, R. M., E. S. Deneris, J. Patrick, and S. Heinemann. The functional diversity of the neuronal nicotinic acetylcholine receptors is increased by a novel subunit: β4. *Neuron* 3:487–496 (1989).
21. Boulter, J., J. Connolly, E. Deneris, D. Goldman, S. Heinemann, and J. Patrick. Functional expression of two neuronal nicotinic acetylcholine receptors from cDNA clones identifies a gene family. *Proc. Natl. Acad. Sci. USA* 84:7763–7767 (1987).
22. Ballivet, M., P. Nef, S. Couturier, D. Rungger, C. R. Bader, D. Bertrand, and E. Cooper. Electrophysiology of a chick neuronal nicotinic acetylcholine receptor expressed in *Xenopus* oocytes after cDNA injection. *Neuron* 1:847–852 (1988).
23. Papke, R. L., J. Boulter, J. Patrick, and S. Heinemann. Single channel currents of rat neuronal nicotinic acetylcholine receptors expressed in *Xenopus* oocytes. *Neuron* 3:589–596 (1989).
24. Bertrand, D., M. Ballivet, and D. Rungger. Activation and blocking of neuronal nicotinic acetylcholine receptor reconstituted in *Xenopus* oocytes. *Proc. Natl. Acad. Sci. USA* 87:1993–1997 (1990).
25. Whiting, P. J., F. Esch, S. Shimasaki, and J. Lindstrom. Neuronal nicotinic acetylcholine receptor β subunit is coded by the cDNA α4. *FEBS Lett.* 219:459–463 (1987).
26. Anand, R., W. G. Conroy, R. Schoepfer, P. Whiting, and J. Linstrom. Neuronal nicotinic acetylcholine receptors expressed in *Xenopus* oocytes have a pentameric quaternary structure. *J. Biol. Chem.* 266:11192–11198 (1991).
27. Cooper, E., S. Couturier, and M. Ballivet. Pentameric structure and subunit stoichiometry of a neuronal nicotinic acetylcholine receptor. *Nature (Lond.)* 350:235–238 (1991).
28. Southern, P. J., and P. Berg. Transformation of mammalian cells to antibiotic resistance with a bacterial gene under control of the SV40 early region promoter. *J. Mol. App. Genet.* 1:327–341 (1982).
29. Saiki, R. H., D. H. Gelfand, S. Stoffel, S. J. Scharf, R. Higuchi, G. T. Horn, K. S. Mullis, and H. A. Erlich. Primer directed enzymatic amplification of DNA with a thermostable DNA polymerase *Science (Washington D. C.)* 239:487–491 (1988).
30. Diehl, R. E., P. Whiting, J. Potter, N. Gee, C. I. Ragan, D. Linemeyer, R. Schoepfer, C. Bennett, and R. A. F. Dixon. Cloning and expression of bovine brain inositol monophosphatase. *J. Biol. Chem.* 265:5946–5949 (1990).
31. Whiting, P. J., R. Schoepfer, W. G. Conroy, M. J. Gore, K. T. Keyser, S. Shimasaki, F. Esch, and J. Lindstrom. Expression of nicotinic acetylcholine receptor subtypes in brain and retina. *Mol. Brain Res.* 10:61–70 (1991).
32. Graham, F. L., and A. J. van der Eb. Transformation of rat cells by DNA of human adenovirus 5. *Virology* 52:456–467 (1973).
33. Wigler, M., A. Pellicer, S. Silverstein, R. Axel, G. Urlabu, and L. Chasin. DNA mediated transfer of the adenine phosphoribosyltransferase locus into mammalian cells. *Proc. Natl. Acad. Sci. USA* 76:1373–1376 (1979).
34. Gough, N. M. Rapid and quantitative preparation of cytoplasmic RNA from small numbers of cells. *Anal. Biochem.* 173:93–95 (1988).
35. Maniatis, T., E. Fritsch, and J. Sambrook. *Molecular Cloning: A Laboratory Manual.* Cold Spring Harbor Laboratory, Cold Spring Harbor, NY (1982).
36. Whiting, P. J., and J. M. Lindstrom. Pharmacological properties of immunoisolated neuronal nicotine receptors. *J. Neurosci.* 6:3061–3069 (1986).
37. Tzartos, S., and J. M. Lindstrom. Monoclonal antibodies used to probe acetylcholine receptor structure: localization of the main immunogenic region and detection of similarities between subunits. *Proc. Natl. Acad. Sci. USA* 77:755–759 (1980).
38. Gorman, C. M., and B. H. Howard. Expression of recombinant plasmids in mammalian cells is enhanced by sodium butyrate. *Nucleic Acids Res.* 11:7631–7648 (1983).
39. Lipiello, P. M., and K. G. Fernandes. The binding of L-^{3}H-nicotine to a single

class of high affinity sites in rat brain membranes. *Mol. Pharmacol.* **29**:448–454 (1986).
40. Martino-Barrows, A. M., and K. J. Kellar. ^{3}H-Acetylcholine and ^{3}H-nicotine label the same recognition site in rat brain. *Mol. Pharmacol.* **31**:169–174 (1987).
41. Marks, M. J., J. A. Stitzel, E. Romm, J. M. Wehner, and A. C. Collins. Nicotine binding sites in rat and mouse brain: comparison of acetylcholine, nicotine and β-bungarotoxin. *Mol. Pharmacol.* **30**:427–436 (1986).
42. Reynolds, J. A., and A. Karlin. Molecular weight in detergent solution of acetylcholine receptor from *Torpedo californica*. *Biochemistry* **17**:2035–2038 (1978).
43. Noda, N., H. Takahashi, T. Tanabe, M. Toyosato, Y. Furutani, T. Hirose, M. Asai, S. Inayama, T. Miyata, and S. Numa. Primary structure of a α subunit precursor of *Torpedo california* acetylcholine receptor deduced from cDNA sequence. *Nature (Lond.)* **299**:793–797 (1983).
44. Mathie, A., D. Colquhoun, and S. G. Cull-Candy. Rectification of currents activated by nicotinic acetylcholine receptors in rat sympathetic ganglion neurones. *J. Physiol. (Lond.)* **427**:625–655 (1990).
45. Ifune, C. K., and J. H. Steinbach. Rectification of acetylcholine elicited currents in PC12 pheochromocytoma cells. *Proc. Natl. Acad. Sci. USA* **87**:4794–4798 (1990).

Send reprint requests to: P. Whiting, Neuroscience Research Centre, Merck Sharp and Dohme Research Laboratories, Terlings Park, Eastwick Road, Harlow, Essex, CM20 2QR UK.